HERIOT-WATT UNIVERSITY

Investigating Hydrocarbon-Degrading Bacteria Associated with Marine Phytoplankton using DNA-Based Stable Isotope Probing

Mohammad Sufian Bin Hudari

Dissertation

Erasmus Mundus Master in Chemical Innovation and Regulation

Work supervised by

Tony Gutierrez

2017

HERIOT-WATT UNIVERSITY

Investigating Hydrocarbon-Degrading Bacteria Associated with Marine Phytoplankton using DNA-Based Stable Isotope Probing

Mohammad Sufian Bin Hudari

Dissertation

Erasmus Mundus Master in Chemical Innovation and Regulation

Work supervised by

Tony Gutierrez

2017

Investigating Hydrocarbon-Degrading Bacteria Associated with Marine Phytoplankton using DNA-Based Stable Isotope Probing

Declaration of Authorship

I declare that I am the author of this work, which is original. The work cites other authors and works, which are adequately referred in the text and are listed in the bibliography.

MOHAMMAD SUFIAN BIN HUDARI

Acknowledgements

Firstly, I thank my supervisor, Tony Gutierrez for giving me this opportunity to partake in research in his lab, as well as his encouragement and support throughout this research project.

I would like to thank Stephen Summers for his support and assistance, and the valuable information and comments in solving lab-related issues.

I thank members of the EMMC-ChIR family especially Professors Emilio Tagliavini, Isabel Cavaco, Teresa Fernandes, and Daniel Sainz for their never-ending support and care throughout the two years of my Masters education. I would also like to thank them for giving me the opportunity to present my research at the annual symposium in Faro. Financial support for this project is deeply acknowledged.

I thank all my colleagues in my lab for their help, Karina Salek in particular, for their friendship and understanding as well as their valuable assistance in the lab. I also thank all my EMMC-ChIR friends, especially Diana Ferrari, Anita Vallejo, and Ester Carregal, for sharing their knowledge, advice, and support during our student life here in Edinburgh.

Special thanks to Pierre Senellart for his patience and support with my endless queries on the LaTeX and TeXnicCenter systems from the start to final revision of the drafts of this thesis.

Lastly, I would like to express my deepest appreciation to my family members for their endless love and support.

Abstract

Marine hydrocarbon-degrading bacteria play an important role in the biodegradation of oil hydrocarbon pollutants in the marine environment. Previous studies have successfully isolated hydrocarbon-degrading bacteria found associated with laboratory cultures of marine phytoplankton. A recent study has shown a dramatic succession of diatom-associated bacterial community, defined by a transition from a short-lived bloom of *Methylophaga* to several groups including hydrocarbonoclastic bacteria on marine diatom *Skeletonema costatum*, in response to crude oil enrichment. However, little is still known about the temporal dynamics of the bacterial symbionts associated with marine phytoplankton and whether *Methylophaga* are directly involved in the degradation of hydrocarbons. In this investigation, DNA-based stable isotope probing (DNA-SIP), which is a valuable tool that allows to link the phylogenetic identity with a specific metabolic function, was employed to identify hydrocarbon-degrading living associated with a laboratory culture of the cosmopolitan marine diatom *Skeletonema costatum* (CCAP 1077/1C). For this, the diatom was enriched with uniformly ^{13}C-labelled *n*-hexadecane as the sole carbon source in a seawater medium. Denaturing gradient gel electrophoresis (DGGE) analysis of 'heavy' DNA at day 8 from the DNA-SIP incubation revealed several distinct bands, that were either not present or whose intensity was less in the 'light' DNA. DGGE analysis of the fractions suggests the presence of several species of hexadecane-degrading bacteria that are living associated with the diatom *Skeletonema costatum*. Future work will explore the phylogenetic identity of the ^{13}C-enriched bacterial community comprising the heavy DNA by barcoded-amplicon Illumina MiSeq sequencing. This work demonstrates the value of DNA-SIP as a sophisticated molecular tool in microbial ecology to identify novel taxa associated with marine phytoplankton and that possesses the ability to perform a target metabolic function – in this case the degradation of hydrocarbons.

Contents

Acknowledgements **1**

Abstract **3**

List of Figures **7**

List of Tables **9**

List of Abbreviations and Acronyms **11**

1 Introduction **13**

1.1 Crude oil in the 21st century 13

1.1.1 Crude oil demand 13

1.1.2 The role of microorganisms in crude oil biodegradation 15

1.2 Stable isotope probing 17

1.3 Objective 17

1.4 Thesis outline 17

2 Background **19**

2.1 Sources of crude oil spills in marine systems 19

2.2 Crude oil composition and characteristics 21

2.2.1 Physical and chemical properties of crude oil 23

2.2.2 Effect of weathering on crude oil in seawater 25

2.3 Diatom-associated bacteria and their role in hydrocarbon degradation . . 30

2.4 DNA-based stable isotope probing 32

3 Experimental methods **35**

3.1 Experimental outline 35

3.2 Materials 36

3.2.1 Strain used 36

3.2.2 Substrate 37

3.3 Methods 37

3.3.1 SIP incubations 37

3.3.2 Measurement of hexadecane degradation 38

3.3.3 Nucleic acid extraction 39

3.3.4 Gradient fractionation and identification of ^{13}C-enriched DNA . . 41

3.3.5 SYBR Safe removal and DNA quantification 42

3.3.6 Denaturing gradient gel electrophoresis 43

4 Results and Discussion **47**

4.1 Degradation of hexadecane during SIP 47

4.2 Nucleic acid extraction of ^{13}C-enriched samples 49

4.3 Separation of 'light' and 'heavy' DNA samples 51

4.4 Quantitative analysis of DNA-SIP gradient fractions 54

4.5 Analysis of the microbial population by DGGE 55

5 Conclusions **61**

5.1 Summary of research achievements 61

5.2 Limitations and shortcomings, and how these were addressed 62

References **67**

List of Figures

1.1 Worldwide energy consumption by fuel type 14

2.1 Examples of hydrocarbon classes 22
2.2 Physical, chemical, and biological processes affecting oil in marine water 26
2.3 Pathways of hydrocarbon degradation 30

3.1 Outline of the DNA-SIP experiment 35
3.2 *Skeletonema costatum* 36
3.3 Ethyl acetate extraction of ^{12}C-enriched and acid-inhibited sets in triplicate test tubes 40
3.4 CsCl ultracentrifugation tubes and ultracentrifuge machine used 43
3.5 DGGE setup 45

4.1 Time course of ^{12}C-hexadecane degradation 48
4.2 DNA isolated 50
4.3 Tube containing ^{13}C-labelled DNA 52
4.4 Gradient fractionation setup 53
4.5 Density measurements for T1A, T1B, T1C and T1D gradient fractions . . 54
4.6 Distribution of the ‘heavy’ and ‘light’ DNA in SIP fractions from samples T1A–T1D 56
4.7 Agarose gel electrophoresis of selected fractions from time point T1D . . 58
4.8 DGGE image of bacterial PCR products from selected fractions from sample T1D 59

List of Tables

1.1 Global consumption of petroleum and other liquid fuels consumption according to region 15

2.1 Types of crude oil and respective constituent classes in weight percentages 23

2.2 Total concentrations of 16 U.S. EPA Priority PAH, aromatic compounds, parent and alkylated PAH, phenanthrene components, and some selected phenanthrene-alkylated derivatives 23

3.1 Physico-chemical properties of hexadecane 37

3.2 Primer used for DGGE-PCR 44

4.1 Cell pellet size comparison 50

4.2 PCR-DGGE selection table 57

List of Abbreviations and Acronyms

API American Petroleum Institute

CsCl cesium chloride

DGGE denaturing gradient gel electrophoresis

DNA-SIP DNA-based stable isotope probing

U.S. EPA United States Environmental Protection Agency

EtBr ethidium bromide

EtOH ethanol

GC-MS gas chromatography mass spectometry

HCB hydrocarbonoclastic bacteria

OPEC Organization of Petroleum Exporting Countries

PAH polynuclear aromatic hydrocarbons

PCR polymerase chain reaction

rpm revolution per minute

SIP stable isotope probing

TAE tris-acetate-EDTA

Chapter 1

Introduction

1.1 Crude oil in the 21st century

Crude oil is an important primary source of energy, and remains the most invested energy commodity in the 21st century (World Bank, Development Prospects Group, 2013; U.S. Energy Information Administration, 2016c). Like many other fossil fuels, crude oil was formed from the decomposition of organic matter under sedimentary rocks, which was subjected to extreme heat and pressure over millions of years. Despite the emergence of novel sources of renewable energy such as solar, wind, and hydro-power, these are considerably far from being economically competitive, given the cost of the technology. Most importantly, crude oil also serves a plethora of other uses beyond being a source of energy. For example, crude oil plays a significant role in the chemical industry as petroleum-based chemical feedstock, lubricants, and wax (U.S. Energy Information Administration, 2016b).

1.1.1 Crude oil demand

Demand for crude oil is expected to increase over time with rising global population. As more countries continue to develop and become more inter-connected, more resources are required to supplement the 'need' for growth (see Figure 1.1). In a study by (Battelle, 2007), it was claimed that two-thirds of refined crude oil were used as fuel in transportation

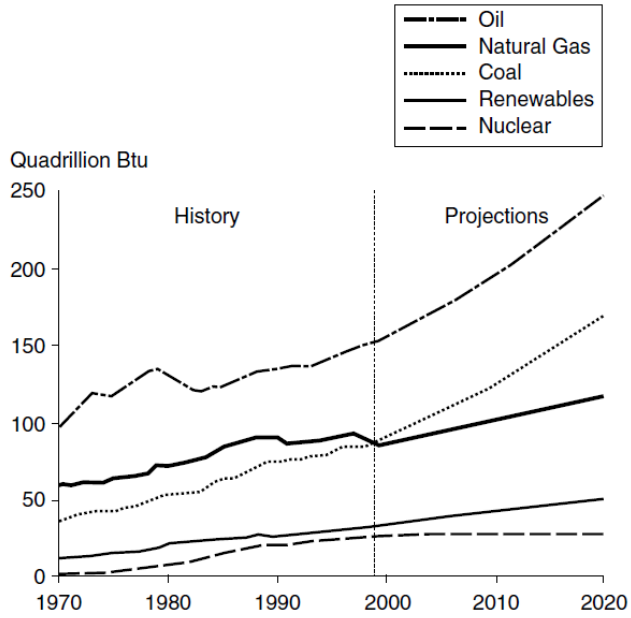

Figure 1.1: Worldwide energy consumption by fuel type (OPEC, 2017)

alone. Latest figures from the Organization of Petroleum Exporting Countries (OPEC) found that the demand for crude oil in 2016 was about 94.44 million barrels per day (Mb/d), which was a year-on-year increase of 1.25 Mb/d; this is expected to increase by another 1.16 Mb/d to about 95.60 Mb/d in 2017 (see Figure 1.1; OPEC, 2017). In order to meet these demands, oil producers are pressured to increase their supply as well as to enhance their extraction capabilities, capacity, and delivery.

Natural oil springs tend to be rare, and hence, most crude oil extraction requires drilling into oil wells. These wells are not distributed uniformly and are likely to be clustered around certain geographical locations located either onshore or close to the shore (Harayama et al., 1999). However, the emerging prospect of abundant supplies of crude oil in the deep and ultra-deepwaters of the continental shelf has driven exploration in uncharted territories in search of new sources of crude oil, coupled also with research in the construction of more robust installations to harvest this novel and untapped resource. With up to 70% of the Earth's surface covered with water and still possibly unexplored, there may be a vast area of potential oil supplies to be discovered. Furthermore, advancement in extraction installation

Table 1.1: Global consumption of petroleum and other liquid fuels consumption according to region (U.S. Energy Information Administration, 2016a)

Region (million barrels per day)	1990	2000	2012	2020	2040
OECD (Total)	42.2	48.7	45.5	45.8	46.1
Americas	20.6	24.3	23.2	24.4	24.6
Europe	14.0	15.6	14.1	13.7	14.0
Asia	7.6	8.8	8.2	7.7	7.5
Non-OECD					
Europe and Eurasia	9.3	4.4	5.3	5.8	6.1
Asia	6.6	12.5	21.5	26.7	38.9
Middle East	3.3	4.5	7.7	10.0	13.2
Africa	2.1	2.5	3.6	4.5	6.9
Americas	3.8	5.0	6.7	7.5	9.6
Total world	67.2	77.7	90.3	100.3	120.9

technologies gives oil producers an added advantage with the extraction platform being mobile, easily transported from one location to another, and having higher extraction efficiency. Moreover, such enhancements in offshore oil extraction technology may make the process more economically viable and, thus, allow oil producers to diversify their sources or enhance their oil reserves (Harayama et al., 1999; ITOPF, 2016).

1.1.2 The role of microorganisms in crude oil biodegradation

Unfortunately, these oil-related activities still pose a threat to the environment, especially pollution from oil spills, even when there have been efforts to step up regulations and remediation control to mitigate its spreading or effect on the ecosystem. While remediation strategies are now more suited to the condition of the spill, its cost and removal efficiency are still challenges that need to be addressed. A report by (Mackelprang & Mason, 2016) suggested that the current combination of mitigation strategies and (non-biological) natural processes may only remove about 78% of the oil, while the rest were believed to have been biodegraded by microorganisms. The role of microorganisms was also supported by (Yang et al., 2016) who postulated that there was likely to be a ‘persistent and widely occurring

seed populations' of microorganisms present in marine water columns that would respond quickly to hydrocarbon enrichment in the water. This was probably based on earlier studies which found that bacteria found in marine systems are likely to be important in the natural attenuation of hydrocarbon (Gutierrez, 2010; Yakimov et al., 2007). In addition, while being enriched in oil impacted environments, marine hydrocarbon-degrading bacteria are believed to be highly specialized in metabolizing hydrocarbon as a carbon and energy source (Gutierrez, 2010; Joye et al., 2016). These seem to indicate that microorganisms play a critical role in the ultimate removal of hydrocarbon from contaminated environment (Gutierrez et al., 2014).

Of late, there has been mounting interest in the role of marine phytoplanktons as a potential biotope for hydrocarbon-degrading bacteria (Mishamandani et al., 2015). This can be exemplified by the discovery of *Polycyclovorans algicola* strain TG408, isolated from the marine diatom *Skeletonema costatum* CCAP 1077/1C. Despite being a specialist hydrocarbon degrader, strain TG408 is not well represented in clone libraries, probably because these organisms occupy a specific niche in the marine environment – i.e., the cell surface of eukaryotic phytoplankton (Gutierrez et al., 2014; Mishamandani et al., 2015). Other studies also found hydrocarbonoclastic bacteria (HCB) residing on the surface of phytoplankton, possibly in a symbiotic relationship (Mishamandani et al., 2015; Gutierrez et al., 2012).

Hydrocarbon enrichment in the cell surface was believed to promote growth of bacterial communities on the cell surface capable of biodegrading hydrocarbon. Cell surface hydrocarbon accumulation could arise from a few probable scenarios: one where the phytoplankton produces hydrocarbons and transports them to the cell surface where these chemicals may accumulate; or probably from the adsorption of hydrocarbons onto the cell surface from the surrounding water (see references in Mishamandani et al., 2015). One of the most commonly used technique to study microbial groups linked to degradation of a specific hydrocarbon is stable isotope probing (SIP).

1.2 Stable isotope probing

SIP allows identification of communities in environmental samples or cultures that may not be amenable to cultivation, by using labelled substrates and investigating their ability to assimilate them (Gutierrez et al., 2015; Whitby et al., 2005). DNA-based stable isotope probing (DNA-SIP), involving DNA as the targeted biomolecule in cells, may be used to assess the catabolic potential of hydrocarbon degraders in ocean systems in order to apply them in future remediation strategies when dealing with oil spill bioremediation. This method avoids the need to isolate the microorganisms while studying their metabolic and physiological characteristics, especially if they cannot be isolated from laboratory cultivation. While DNA-SIP has allowed hydrocarbon-degrading bacteria that are associated with phytoplankton to be studied extensively, there is still little information on how these microbial community present on the surface of phytoplanktons change over time when enriched with substrates. Therefore, we aim to study how communities of diatom-associated hydrocarbon-degrading bacteria evolve over time and, specifically, to target the identification of hydrocarbon-degrading bacteria living associated with phytoplankton. In particular, we were interested to determine if members of the genus *Methylophaga*, which are known to utilise C1 carbon substrates, such as methanol, might also be found and capable of degrading the hydrocarbon *n*-hexadecane, the substrate selected for this study.

1.3 Objective

In this study, DNA-SIP was employed to target the identification of hydrocarbon-degrading bacteria living associated with the marine diatom *Skeletonema costatum*, as well as to assess its dynamics in this enrichment experiment with uniformly labelled *n*-hexadecane.

1.4 Thesis outline

This thesis is divided into five chapters. This chapter described the background and importance of crude oil in the society, and how its demand serves as the driving force

behind the extensive offshore exploration in the world's oceans. Oil-related activities still remain a cause of environmental concerns such as oil pollution in marine waters. The present chapter also briefly described the potential role of microorganisms in the removal of crude oil hydrocarbon from marine ecosystems while introducing the essential concept of diatom-associated bacteria, its role as a biotope for hydrocarbon-degrading bacteria and how DNA-based stable isotope probing is a valuable tool in this respect. Chapter 2 provides an overview on the background and concepts related to oil pollution such as the composition of crude oil and effects of weathering on crude oil when a spill occurs. Details on the experimental study is described in Chapter 3. Chapter 4 presents and discusses the results of the DNA-SIP experiment. Finally, Chapter 5 concludes this report by describing the challenges and limitations faced in this study and by proposing recommendations on future experiments and analysis.

Chapter 2

Background

2.1 Sources of crude oil spills in marine systems

Sources of oil spills can either be natural or anthropogenic, acute or chronic. Regardless, their effects may be long-lasting and detrimental to the ecosystem. It is worth noting that while a spill may be acute, the presence of high levels of persistent compounds such as polynuclear aromatic hydrocarbons (PAH) can still be toxic to marine organisms (Battelle, 2007). Organisms may also experience chronic exposure, when oil is released over extended periods of time, albeit in small amounts. Examples of chronic exposures are natural seeps (from a natural source) and a leaking pipeline (anthropogenic release). In both cases, factors such as volume, area, and location of the spill, as well as the sensitivity of organisms and whole ecosystems to heightened levels of hydrocarbon pollutants in the water are critical to determining the impact of the exposure on the surrounding ecosystems (Head et al., 2006; Gutierrez, 2010).

Sources of oil input can be categorized into four groups: natural seeps, petroleum extraction, petroleum transportation, and petroleum consumption (Transportation Research Board and National Research Council, 2003; Steering Committee for the Petroleum in the Marine Environment Update, National Research Council, 1985; IARC Monographs, 1989). Their combined release amounted to 1,300,000 tonnes of petroleum into marine waters globally (Transportation Research Board and National Research Council, 2003).

Natural seeps in the marine environment tend to originate from geologic formations below the seafloor. These have been estimated to exceed 600,000 tonnes, constituting 45% of the petroleum entering marine waters globally (Transportation Research Board and National Research Council, 2003). Oil slicks from seeps tend to be associated with gas and oil platform since they are located close to regions where these seeps occur, often used as indicators of presence of petroleum reserves such as those seen found in the Gulf of Mexico (Transportation Research Board and National Research Council, 2003).

Petroleum extraction, transportation, and consumption comprise most of the anthropogenic sources of oil pollution, accounting to about 54% of the remaining petroleum releases. Of this 37% are due to consumption activities, 12% from transportation operations, and 3% from extractions (Transportation Research Board and National Research Council, 2003; Steering Committee for the Petroleum in the Marine Environment Update, National Research Council, 1985; Office of Response and Restoration, National Oceanic and Atmospheric Administration, University of Toledo, 2015).

Crude oil extraction may release both crude oil and drilling products, which are likely to be found near active exploration sites (e.g., spills from the 2010 Deepwater Horizon blowout) (Office of Response and Restoration, National Oceanic and Atmospheric Administration, University of Toledo, 2015).

Tankers and pipelines are the main modes of oil transportation, and these spills may occur on a large scale (e.g., Exxon Valdez tanker spill) or on a small scale (e.g., operational spills) (IARC Monographs, 1989).

However, the largest percentage of anthropogenic oil releases come from petroleum consumption. Examples of releases coming from petroleum consumption include operational discharges and recreational boating. It is crucial to understand that types of compounds released into the environment depend on various factors such as sources and types of input, as well as the activity, and process involved. Hence, it is important to study what constitutes crude oil in order to predict its behaviour and fate in the environment.

2.2 Crude oil composition and characteristics

Crude oil composition varies with location and the geological formation from which it was formed. Chemically, it can be categorized into hydrocarbon and non-hydrocarbon constituents. Hydrogen and carbon constitutes up to 97% of crude oil, either as hydrocarbon or hydrocarbon-related compounds while the rest is made of non-hydrocarbon components such as nitrogen, sulfur, oxygen, minerals, and trace metals such as vanadium and chromium (Transportation Research Board and National Research Council, 2003; Steering Committee for the Petroleum in the Marine Environment Update, National Research Council, 1985). Hydrocarbon components may also be classified based on their structures which could influence their fate and effect when they enter the environment. In general, saturates, olefins (now called alkenes), aromatics, and polar compounds comprise crude oil hydrocarbon, though they are usually categorized under four classes of compounds: saturates, aromatics, resins, and asphaltenes (Transportation Research Board and National Research Council, 2003; Steering Committee for the Petroleum in the Marine Environment Update, National Research Council, 1985), see Figure 2.1.

Saturates are a class of hydrocarbon comprising alkanes and cycloalkanes. They possess a carbon 'backbone' containing the maximum number of possible hydrogen bonded to it and thus are 'saturated'. The general formula for alkanes are (C_nH_{2n+2}) (IARC Monographs, 1989). Alkanes form the main bulk of this group. Cycloalkanes are structures of carbon atoms which are bonded to each other to form rings saturated with hydrogen atoms. High molecular weight saturates are usually called 'waxes' (Transportation Research Board and National Research Council, 2003; Steering Committee for the Petroleum in the Marine Environment Update, National Research Council, 1985).

Alkenes, in contrast, are 'unsaturated' as they possess fewer hydrogen atoms than the maximum number of hydrogen possible. The general formula for alkenes are (C_nH_{2n}) with at least a single carbon to carbon double bond present.

Aromatics are relatively stable compounds with at least one benzene ring (IARC Monographs, 1989). Benzene rings, owing to their stability, tend to be more persistent in the environment and potentially toxic to certain organisms. Aromatic hydrocarbons may con-

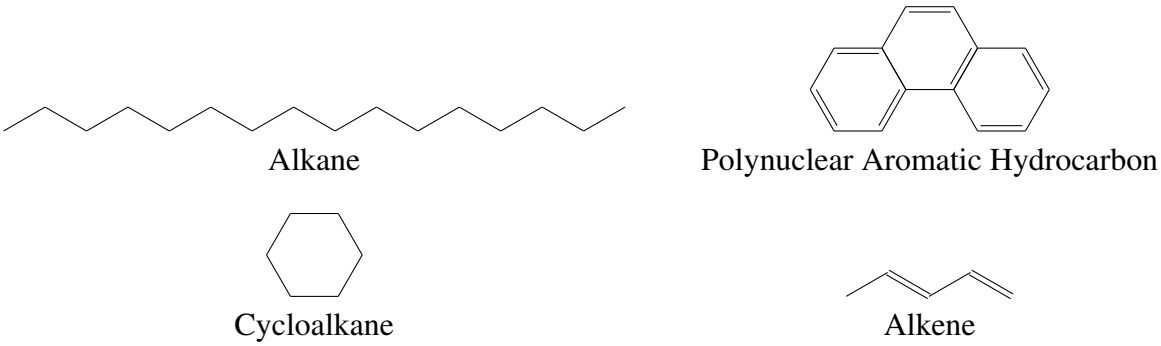

Figure 2.1: Examples of hydrocarbon classes

stitute between 1 and 20% of the total hydrocarbons present in crude oil (Transportation Research Board and National Research Council, 2003). PAH contain multiple rings, usually at least two benzene rings. It is estimated that the total PAH in a typical crude oil constitutes between 0.2 to more than 7 percent (Transportation Research Board and National Research Council, 2003). PAH can either be homocyclic (purely hydrogen and carbon based) or heterocyclic where it can contain other elements such as nitrogen, sulfur and oxygen. Aromatic hydrocarbons tend to be less abundant with increasing molecular weight. Homocyclic aromatic hydrocarbons which consist of one (e.g., benzene) to three rings (e.g., phenanthrene) and heterocyclic aromatic rings (e.g., dibenzothiopene) make up to at least 90% of the aromatic hydrocarbon present (Transportation Research Board and National Research Council, 2003). PAH are considered to be the most detrimental to the environment with many of them listed on the Environment Protection Agency (EPA) Priority Pollutant List, such as anthracene and phenanthrene (United States Environment Protection List, 2014).

Polar crude oil components bear a resultant molecular charge resulting from bonds formed with electronegative elements such as oxygen, sulfur and nitrogen. Within this class, smallest polar compounds are referred to as resins while the larger ones are termed asphaltenes (Transportation Research Board and National Research Council, 2003).

Crude oil can also be categorized depending on the relative abundances of each of the four classes of compounds. These four types of crude oil: light, medium, heavy crude, and

Table 2.1: Types of crude oil and their respective constituent classes in weight percentages (National Academies of Sciences, Engineering, and Medicine, 2016; Hollebone, 2014)

Type of crude oil	Saturates	Aromatics	Resins	Asphaltenes
Light crude[a]	92	8	1	0
Medium crude[b]	78	15	6	1
Heavy crude[c]	38	29	20	13
Diluted bitumen[d]	25	22	33	20

[a] Scotia Light [b] West Texas Intermediate [c] Sockeye Sour [d] Cold lake blend

Table 2.2: Total concentrations of 16 U.S. EPA Priority PAH, aromatic compounds, parent and alkylated PAH, phenanthrene components, and some selected phenanthrene-alkylated derivatives (concentration values in µg/g) (National Academies of Sciences, Engineering, and Medicine, 2016; Hollebone, 2014)

Type of crude oil	Light	Medium	Heavy	Diluted Bitumen
Sample	Scotia Light	West Texas	Sockeye	Diluted Bitumen
Total 16 U.S. EPA PAH	139	514	218	176
Total Aromatic Compounds	3,504	7,947	5,231	5,384
Total parent & alkylated PAH	3,434	7,841	5,147	5,326
Sum of phenanthrene and its alkylated derivatives (C0–4)	351	1,295	1,078	1,242

diluted bitumen, vary by weight percentages in saturates, aromatics, resins, and asphaltenes contents (see Tables 2.1 and 2.2).

2.2.1 Physical and chemical properties of crude oil

Several factors may affect the behaviour and fate of crude oil components in the event of an oil spill: viscosity, relative density (specific gravity), solubility, distillation characteristics, and pour point (Transportation Research Board and National Research Council, 2003; ITOPF, 2011). These properties are related to the chemical composition of the crude oil.

Viscosity refers to the resistance of a liquid to flow. A low-viscosity liquid tends to flow more readily. Oil viscosity is determined by the proportion of light to heavy fractions. Therefore, oil comprising a high percentage of lighter fraction oil and a low percentage of heavy fraction oil would be less viscous. Low-viscosity oil tends to spread easily and

is more prone to weathering, while viscous oil tends to form tarballs and is likely to accumulate into thick deposits (Transportation Research Board and National Research Council, 2003).

Density is defined as the mass of a given volume of oil (in g/cm^3), which can be used to determine the types of crude oil. Specific gravity or relative density refers to the density of crude oil with respect to pure water, which has a specific gravity of 1 (ITOPF, 2011) Specific gravity determines if the oil or its constituents float or sink in seawater. The API scale, a commonly used gravity scale devised by the American Petroleum Institute (API) to 'quantify' the specific gravity of crude oil and petroleum products. Oil has a density between 0.7 to 0.99 g/cm^3 (at 15°C) which is less dense than water ($1.0\,g/cm^3$). Seawater has a specific gravity of 1.025 and is therefore denser than pure water. Therefore, most range of oil tends to float on the surface of seawater (Transportation Research Board and National Research Council, 2003; ITOPF, 2011). Lighter oil fractions may evaporate more readily or possibly get biodegraded, leaving the majority of the heavier fractions of oil which are most likely to be more persistent in the environment. Therefore, the API scale can also be used to predict if the oil possesses a high proportion of volatile compounds.

Solubility refers to the extent to which oil molecules dissolve in water. It is important to note that while the solubility of oil is estimated at about 100 parts per million (ppm), the water soluble fraction can still be toxic to aquatic organisms.

Distillation characteristics describe how volatile the oil is. This is assessed through a distillation process, by analysing the boiling and condensation patterns of the components which are represented proportionally to that of the parent oil (ITOPF, 2011). Oil comprising large amounts of asphaltenic components are unlikely to distil at high temperature and more likely to be persistent in marine environments.

Pour point of crude oil depends on the proportion of wax and asphaltene. This property affects the temperature below which oil ceases to flow. Hence, when oil cools, it becomes more viscous until it reaches the cloud point. At this stage, the wax component starts forming crystalline structures and further impedes oil flow until pour point is reached and the oil stops flowing and becomes semi-solid (ITOPF, 2011).

2.2.2 Effect of weathering on crude oil in seawater

Weathering is used to describe the combined processes which involve the biological, chemical, and physical changes to oil upon entering seawater (U.S. Congress, 1991). These processes occur at varying rates and are highly temperature-dependent, but tend to be highest immediately after release. Processes which are considered crucial in weathering include evaporation, dissolution, biodegradation, and photooxidation (Liu et al., 2012). However, other processes which may also contribute to weathering are spreading, dispersion, sedimentation, emulsification, and oxidation.

This section provides a brief overview of the processes that affect the fate of oil in seawater.

Evaporation Evaporation occurs when molecules of a liquid which are close to the surface attain enough energy to overcome intermolecular attractions to escape from the bulk of the liquid into the vapour phase. The rate of evaporation depends on several factors: temperature, attractive forces between the molecules in the liquid, surface area, and pressure over the liquid, oil composition, surface area, wind velocity, air and sea temperature (Raj, 2009; U.S. Congress, 1991). This process is considered to be the most crucial weathering phenomenon in the initial 48 hours of an oil spill, with substantial losses in low-to medium weight components with low boiling points (U.S. Congress, 1991). The resultant oil spill, however, becomes more viscous and denser.

Spreading Oil tends to spread on water surfaces to form a thin film if left unconstrained and increases the surface area of oil on the surface (National Academies of Sciences, Engineering, and Medicine, 2016). While spreading increases the footprint of oil in the environment, it is more prone to photooxidation and evaporation (National Academies of Sciences, Engineering, and Medicine, 2016).

Dissolution Dissolution may occur as long as a crude oil constituent is at least slightly soluble in water. Several factors tend to influence the rate and extent of dissolution such as oil composition, temperature, spreading and degree of dispersion (ITOPF, 2011). Losses

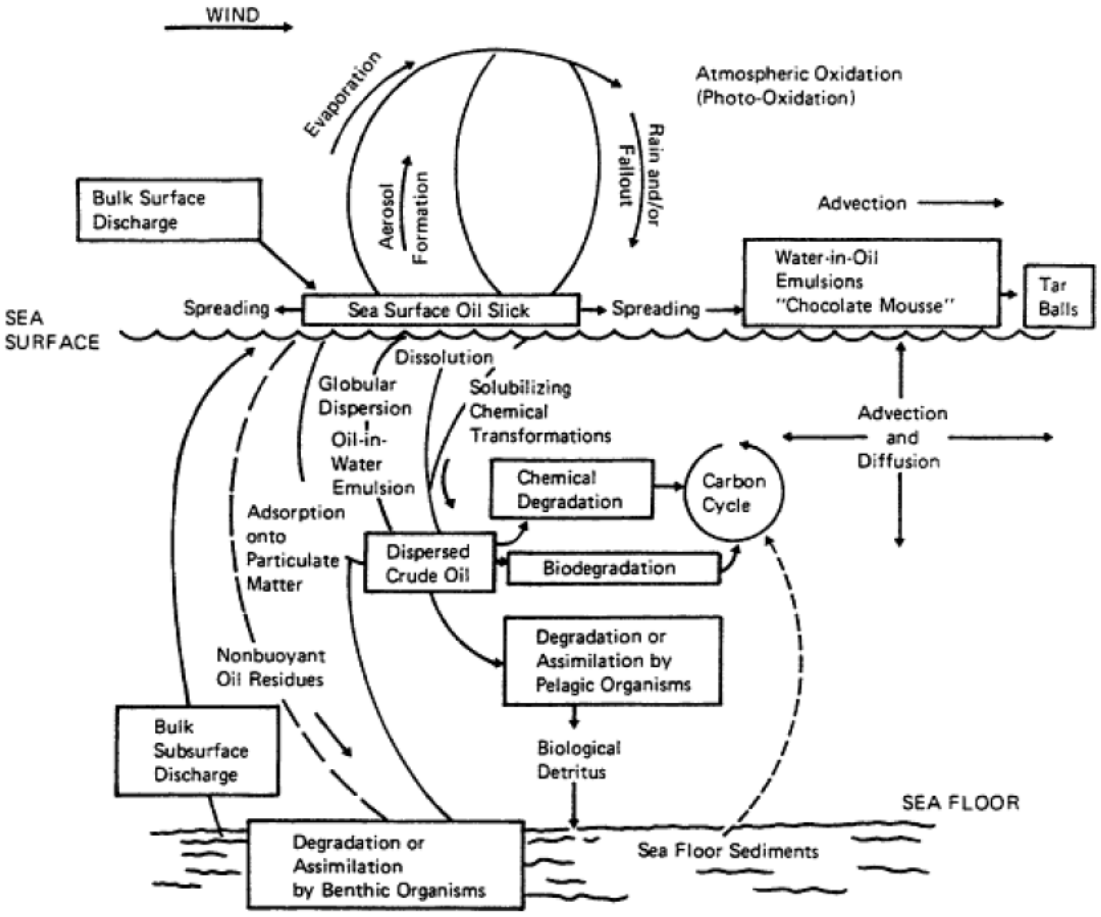

Figure 2.2: Physical, chemical, and biological processes affecting oil in marine water (Steering Committee for the Petroleum in the Marine Environment Update, National Research Council, 1985)

through dissolution are considerably less important than evaporative losses but these soluble components can still be toxic to the marine organisms (U.S. Congress, 1991).

Oxidation and photooxidation Hydrocarbon oxidation involves reaction with oxygen to form products that are either more soluble or more persistent (ITOPF, 2011). Photooxidation is an oxidation process that is promoted by sunlight and may result in oxygen incorporated into the molecules. Carbon dioxide and other oxygenated products are amongst some products of oxidation reactions (Aeppli et al., 2012; Prince et al., 2003; National Academies of Sciences, Engineering, and Medicine, 2016). Aromatic hydrocarbons tend to be oxidized more readily than linear alkanes while branched chained alkanes tend to be photooxidized the slowest (D'Auria et al., 2009; National Academies of Sciences, Engineering, and Medicine, 2016). However, removal by photooxidation is not as significant as other weathering processes even though there is a probability that photooxidation products may be more persistent than their parent compounds (ITOPF, 2011).

Dispersion Dispersion occurs when oil droplets get entrained in the water column. The extent of oil dispersion depends on the inter-facial tension between oil and water, oil viscosity, and the mixing energy that may be driven by wind, current, or tides (ITOPF, 2011). Despite this, inter-facial tension between oil and water does not vary widely among oil types.

Chemical dispersants can be used to decrease inter-facial tension by 10–200 fold, allowing a greater proportion of oil to disperse into the water column (ITOPF, 2011). This is therefore important when removing oil slick from the surface of water bodies (U.S. Congress, 1991). Droplet size distribution of oil dispersed in water plays an important role in the behaviour of oil in the aquatic environment. Larger droplets are more buoyant than smaller droplets and likely to rise to the water surface, regardless whether they are released underwater or released on the water surface and entrained into the water column by turbulence (National Academies of Sciences, Engineering, and Medicine, 2016). Smaller droplets have a larger surface area for other weathering effects to take place.

Emulsification Emulsification is the process when one liquid is dispersed into another, in small droplets and becomes physically stable. It is often considered synonymous with dispersion. Oils that form stable water-in-oil emulsions may contain as much as 70–80% water. This stability also reduces the effects of other weathering processes resulting in a compound that is highly persistent (ITOPF, 2011).

Sedimentation Sedimentation can occur if entrained oil droplets adhere to suspended sediments forming of oil-particle aggregates that settle out of the water column. For example, light oil that has a specific gravity lesser than sea water stays afloat, but when adhered onto dense materials, causes it to sink if the specific gravity becomes substantially high.

Biodegradation Hydrocarbon biodegradation involving living organisms, typically bacteria, is by far one of the most crucial modes in the removal of oil hydrocarbon from marine systems (Prince et al., 2003; Harayama et al., 1999; U.S. Congress, 1991). Biodegradation can occur both aerobically and anaerobically; however, the rate and extent of degradation are influenced by the characteristics of the oil, temperature, and oxygen and nutrient availability (ITOPF, 2011). Anaerobic degradation of hydrocarbon has also been reported though it occurs at a much slower rate and the pathways remain unclear. Therefore, most studies are usually focused on the aerobic degradation of crude oil.

Smaller molecular weight saturates and aromatics comprising up to three aromatic rings tend to be biodegraded more readily, while compounds with four or more aromatic rings are less susceptible to biodegradation, and therefore more persistent in the environment (Harayama et al., 1999; U.S. Congress, 1991). *n*-Alkanes, cycloalkanes, and PAH also undergo aerobic degradation more readily. Biodegradation of the crude oil hydrocarbon typically produces carbon dioxide and water as the by-products which are non-toxic and safe. Therefore, bioremediation of hydrocarbon-polluted waters are seen as a more environmentally viable and less costly option when compared to other remediation methods.

There have been substantial studies highlighting the ability of microorganisms to utilize crude oil components as substrates in marine systems (Fathepure, 2015). Many of these microorganisms were believed to have adapted to be able to utilize these substrates over millions of years, likely from chronic exposure to naturally occurring oil releases such as cold seeps (McGenity et al., 2012). This enables them to adapt to survive in oil polluted environments by diversifying their source of carbon and energy. It was found that at least 175 genera of bacteria, several haloarchaeal genera, as well as eukarya possess this ability to transform or grow on hydrocarbons (McGenity et al., 2012; Fathepure, 2015). Several reports found microorganisms (e.g., *Alcanivorax*) that are present and potentially important in petroleum biodegradation (Harayama et al., 1999; Yakimov et al., 2007; Kostka et al., 2011). Most of the time, these microorganisms tend to be specialist degraders, in that they only metabolize a certain group or hydrocarbons; but it was also reported that different types of degraders may work together or in succession to degrade different oil components (ITOPF, 2011).

For biodegradation to be possible, the microorganism must possess enzymes that are capable of catalysing hydrocarbon degradation. In general, these enzymes attempt to make hydrocarbons more soluble by adding oxygen to the molecules. This may occur via a metabolic pathway involving a consortium of enzymes. For instance, *Pseudomonas putida* possesses the OCT plasmid which allows it to degrade *n*-alkanes by first oxidizing the terminal methyl group via alkane hydroxylase, producing *n*-alcanols (Harayama et al., 1999). This is further oxidized to *n*-alkanals by alcohol dehydrognenase before being further converted to fatty acids by aldehyde dehydrogenase and finally to acyl-CoA by acyl-CoA synthetase.

While the desired products of biodegradation are carbon dioxide and oxygen, this depends on the degradation pathway in each organism. There are also other pathways for the degradation of cycloalkanes, branched alkanes, and other hydrocarbons (see Figure 2.3). For instance, degradation of simple PAH may begin with the dihydroxylation of one of the polynuclear aromatic rings, which is later cleaved. This cleaved ring is then ‘removed’ before the second ring (Harayama et al., 1999). Asphaltenes and resins may still be

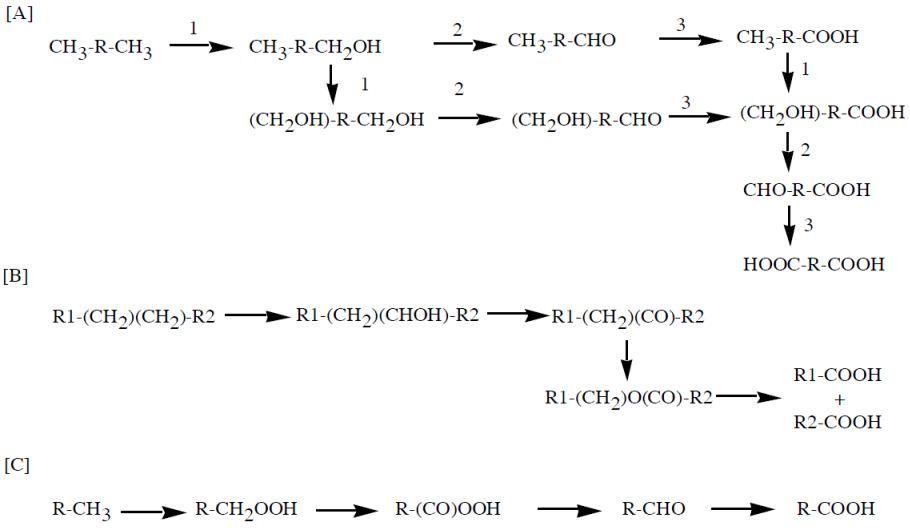

Figure 2.3: Possible pathway of hydrocarbon degradation (Harayama et al., 1999). [A] Terminal oxidation of n-alkanes in bacteria; steps 1, 2 and 3 are catalysed by different enzymes. [B] Subterminal oxidation of n-alkanes. [C] n-Alkane degradation via the alkyl hydroperoxide pathway.

biodegradable if the conditions are feasible, even though they are regarded as highly recalcitrant to biodegradation (Rontani et al., 1985; Harayama et al., 1999).

2.3 Diatom-associated bacteria and their role in hydrocarbon degradation

Marine phytoplankton are gaining more interest because they may be a niche for potentially novel bacteria communities that could play a significant role in hydrocarbon degradation. Diatoms, one of the most common types of marine phytoplankton, are photosynthetic eukaryotes found in large abundance in oceans and account for 20% of the photosynthesis on Earth (Amin et al., 2012). They are crucial as primary producers in the food chain and plays an important role in transporting fixed organic carbon from the upper layer of the aquatic system to deeper layers when they die and sink (Amin et al., 2012). Diatoms are also unique in that most of them require silicon in the form of silicate SiO_4^{2-} for the synthesis of glass-like 'shells' called frustules, even though there are exceptions,

such as *Phaeodactylum tricornutum* that do not necessarily require silicon for frustule formation (Amin et al., 2012; Verlencar & Desai, 2004). Phytoplankton are enveloped by a phycosphere which is a region that surrounds the algal cell or groups of cells which could host bacterial communities promoted by extracellular products of the alga, analogous to rhizospheres in soil ecosystems (Amin et al., 2012). This thin diffusive boundary layer surrounding the cell does not mix with the surrounding fluid and may be suitable for accumulation of certain chemical compounds (Amin et al., 2012).

Studies have shown that eukaryotic phytoplankton can produce extracellular polymeric substances (EPS) either on their cell surface or into the surrounding seawater (Gutierrez et al., 2014; Amin et al., 2012). A study by Binark et al. (2000) also observed that marine algae could adsorb up to 14 distinct types of PAH. Other studies have also demonstrated the potential of marine phytoplankton to adsorb and concentrate PAH from the surrounding water (Andelman & Suess, 1970; Gutierrez, Green, et al., 2013). Hydrocarbon accumulation in the phycosphere thus serves as a potential biotope for hydrocarbon-degrading bacteria which may become associated with the phytoplankton. A microbial shift in the communities that are dominating the phycosphere at any one time seems highly probable, given the availability of carbon as a source of energy and biomass with different types of hydrocarbon potentially accumulating in the phycosphere of the diatom. For example, hydrocarbon-degrading bacteria associated with marine phytoplankton have recently been discovered amongst these communities (Gutierrez, Green, et al., 2013; Mishamandani et al., 2015; Gutierrez et al., 2014). While it was found that the hydrocarbon-degrading phenomenon could exist in in the absence of the alga, the bacteria-diatom association could facilitate the hydrocarbon uptake in the marine environment, potentially playing an important role in hydrocarbon removal from marine systems. (Gutierrez et al., 2014). Unfortunately, much is still unknown about these diatom-associated microbial dynamics.

2.4 DNA-based stable isotope probing

DNA-SIP can assist in linking the phylogeny of organisms to their function when the organisms incorporate the substrates within their DNA (Neufeld, Vohra, et al., 2007). This has been demonstrated successfully with the characterisation of the bacterial taxa involved in the biodegradation of environmental contaminants in various environmental partitions (Gutierrez, Green, et al., 2013; Cheng et al., 2013).

Stable-isotope probing (SIP) serves to characterize individual organisms that are capable of metabolizing a specific substrate without the need to enrich or isolate them on a selective media containing the substrate. This can also be implemented without prior knowledge of the organisms responsible for the biodegradation of the contaminant, and be tested on any type of contaminant, provided that isotopic forms of the target substrate are available (ITRC, 2011; Gutierrez et al., 2015).

DNA-based SIP is based on the fact that when microorganisms grow and multiply, they have to synthesize new biomolecules (e.g., nucleic acids, proteins, and lipids) which contain carbon – in this case DNA. These biomolecules are obtained from the degradation of chemicals derived from the environment. When the microorganisms grow and divide, these simple metabolites are assimilated and therefore reflect any isotopic composition of the chemicals which the microorganisms are exposed to. For example, if microorganisms are grown on substrate comprising entirely of ^{12}C (the most abundant isotope of carbon), then every carbon atom in the newly formed DNA would consist of ^{12}C. However, if the microorganisms are exposed to ^{13}C-labelled substrates, then a similar outcome would be expected, with every carbon atom in the new DNA made up of ^{13}C. This phenomenon is exploited in DNA-SIP, which involves exposing samples to isotopically enriched substrate. After a predetermined period of time, all the nucleic acid is extracted from the sample and analysed. If biodegradation of the substrate does occur, then some of the extracted DNA will contain the stable isotope present in the substrate. With no other significant pathway for assimilation of substrate to DNA, then biodegradation of the substrate by the microorganism is likely.

SIP can be done using ^{13}C, ^{15}N, and ^{18}O although most studies use ^{13}C-labelled compounds. However, SIP experiments depend on the availability of isotopically enriched forms of the contaminants and the ability to obtain the target compounds which have been substantially labelled with the stable isotope of choice (Neufeld, Wagner, & Murrell, 2007). Nonetheless, there has since been numerous applications of SIP to important contaminants. For instance, SIP has been applied to a variety of contaminants such as benzene, toluene, polychlorinated biphenyls, and uranium (ITRC, 2011).

In DNA-SIP experiments, DNA that has been labelled with the stable isotope, for example ^{13}C, can be separated from DNA containing ^{12}C by density-gradient centrifugation. This is because, while the buoyant density of DNA varies with its GC (guanine and cytosine) content, the incorporation of ^{13}C into the DNA further enhances this density difference. With the addition of nucleic acid stain such as ethidium bromide, two bands would be visible under ultraviolet (UV) illumination, with the first band lower in the tube from the heavy ^{13}C-labelled DNA and the upper band from the non-enriched ^{12}C-labelled DNA. Other nucleic acid stain such as SYBR Safe™ and illumination method such as blue light transilluminator have since been proposed as safer alternatives to ethidium bromide and UV light respectively and eventually replaced (Martineau et al., 2008).

While the first DNA-SIP experiments involved one-carbon compound as substrates (e.g., $^{13}CH_3OH$), it is now possible to obtain complex compounds that have been entirely labelled with ^{13}C such as uniformly labelled ^{13}C-hexadecane, which was selected as the substrate for this study. Several studies have also successfully characterized bacteria involved in hexadecane degradation in several studies in DNA-SIP experiments using ^{13}C-hexadecane (Cheng et al., 2013; Mishamandani et al., 2014).

Chapter 3

Experimental methods

This study aims to identify the hexadecane-degrading microbial community associated with the diatom *Skeletonema costatum*. The first setup measures hexadecane degradation over predetermined time points; in a separate setup, incubation flasks involving ^{13}C isotope-labelled *n*-hexadecane (DNA-SIP incubation) are sacrificed and their community analysed.

3.1 Experimental outline

In general, DNA-SIP involves three major steps (Chen et al., 2010): (i) incorporating the stable ^{13}C-isotope labelled substrate into the sample as a tag; (ii) separating the

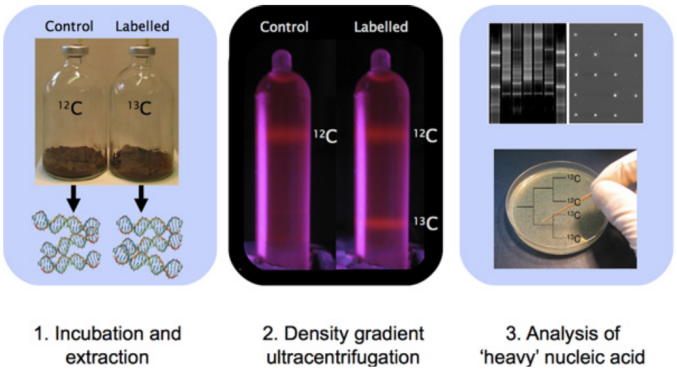

Figure 3.1: DNA-SIP experimental outline (Dunford & Neufeld, 2010)

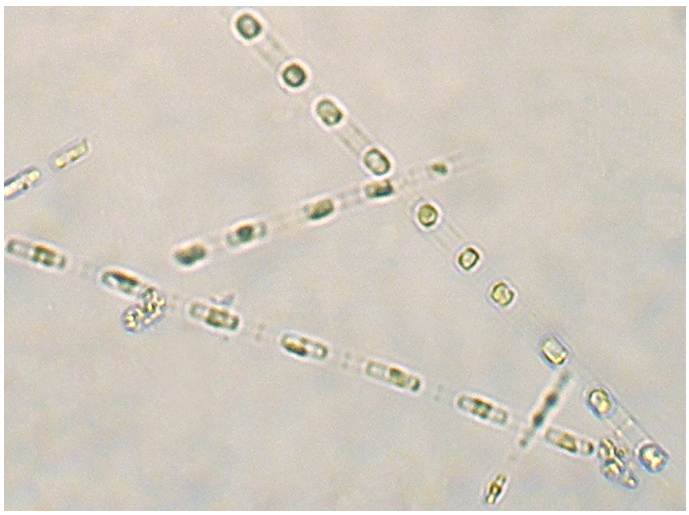

Figure 3.2: *Skeletonema costatum* (CC-BY-SA 3.0, Minami Himemiya)

labelled ^{13}C and unlabelled ^{12}C substrates by ultracentrifugation; and (iii) analysing the ^{13}C-labelled DNA.

3.2 Materials

3.2.1 Strain used

Marine diatom *Skeletonema costatum* CCAP 1077/1C, pictured in Figure 3.2, was obtained from the Culture Collection of Algae and Protozoa (CCAP, Scotland), from an unspecified area in the North Sea. *Skeletonema costatum* have cylindrical cells with round ends, forming long straight chains that are held by fine tubular processes which are parallel to the longitudinal axis (Spaulding & Edlund, 2008). This strain has been selected as a model organism because of its tolerance to variable light regimes and temperature, tendency to dominate diatom abundance in coastal waters, and is commonly used to assess non-toxic bloom management given its rapid growth and high population densities (Kumar & Prabu, 2014). More importantly, *Skeletonema costatum* was selected because studies (Gutierrez et al., 2014; Mishamandani et al., 2015) have shown that it harbours novel bacterial species that can degrade hydrocarbon. *Skeletonema costatum* was maintained in non-axenic lab cultures of F/2 + Si algal medium containing sterile inorganic nutrients, trace metal and

Table 3.1: Physico-chemical properties of hexadecane (National Center for Biotechnology Information, 2017)

property	hexadecane
molecular formula	$C_{16}H_{34}$
skeletal formula	
type of hydrocarbon	Aliphatic
molecular weight	226.488 g/mol
density	0.77335 at 20°C
melting point	18.14°C
boiling point	286.5°C
vapour pressure	1 mmHg
solubility in seawater	4×10^{-5} mg/L at 25°C
$\log K_{o/w}$	8.25

vitamin solutions under conditions recommended by (Guillard, 1975; Guillard & Ryther, 1962).

3.2.2 Substrate

We have selected *n*-hexadecane as the model substrate for this study as it has been used as a representative aliphatic hydrocarbon component of crude oil in several studies (Cheng et al., 2013; Marchant et al., 2006). See Table 3.1 for a summary of physico-chemical properties of hexadecane.

3.3 Methods

3.3.1 SIP incubations

In incubations involving ^{13}C-labelled substrates, the sample must be labelled substantially with ^{13}C to target only the primary consumers of the substrate while avoiding any cross-feeding of the heavy-isotope labels. Therefore, an appropriate concentration of substrate must be selected so that it is neither toxic nor inhibitory to the microorganisms, and more

importantly, to ensure that substrates are not partially labelled, so as to allow separation of 'heavy' from 'light' DNA (Chen et al., 2010).

SIP incubations were conducted similar to that described by Gutierrez, Singleton, et al. (2013), using 10 autoclaved 250-mL Erlenmeyer conical flasks with sponge bungs. Each flask contained 45 mL of enriched seawater media F/2 + Si, 8 µL of *n*-hexadecane (labelled ^{13}C or unlabelled ^{12}C), and 5 mL of inoculum. We purchased [U-^{13}C] *n*-hexadecane from Sigma-Aldrich (United States). Flasks were divided into three sets: ^{13}C-enriched, ^{12}C-enriched, and acid-inhibited control. The ^{12}C-enriched and acid-inhibited control sets were ran in triplicates (for ^{12}C-enriched and acid-inhibited control incubations) while the four remaining flasks were used as replicates for DNA-SIP incubation (^{13}C-enriched). All three sets of flasks were run in parallel at 25°C in the dark.

The ^{12}C-enriched and acid-inhibited control triplicate sets were used to monitor the disappearance of the substrate by gas chromatography mass spectometry (GC-MS), with the acid-inhibited triplicate set used as the negative control. The first set of triplicate flasks (^{12}C-enriched) was prepared by adding 8 µL of unlabelled ^{12}C-hexadecane into each flask. The second set (acid-inhibited control) containing unlabelled ^{12}C-hexadecane was prepared by adding 85% phosphoric acid (ca 2 mL per flask) to pH < 2.

The ^{13}C-enriched set, which is the DNA-SIP set, consists of four replicate flasks. For this, the flasks were each sacrificed on days 2, 3, 6, and 8 by centrifuging contents of the entire flask to obtain cell pellets which were later used for the subsequent DNA extraction, isopycnic ultracentrifugation of the 'heavy' DNA and subsequent molecular analysis. Each time point was labelled as T1A, T1B, T1C, and T1D to represent days 2, 3, 6, and 8 at which the flasks were sacrificed respectively. These labels will be used throughout this study for easier reference.

3.3.2 Measurement of hexadecane degradation

Measurements are used to assess the hexadecane-degrading ability of the bacterial community associated with *Skeletonema costatum* strain CCAP 1077/1C.

During sampling, 1 mL of sample was transferred from each flask from the ^{12}C-enriched and acid-inhibited sets over predetermined days into acid-washed, screw-top test tubes. 2 mL of ethyl acetate (HPLC grade) was then added into each tube and vortexed for about 30 s. The tubes were stored at 4°C until GC-MS analysis (see Figure 3.3). For this, 1–2 mL of the upper organic phase was transferred into screw-cap vials and sent for GC-MS at Heriot-Watt University. During analysis, 50 µL of sample was transferred into a 20 mL screw topped vial containing 4.75 mL of deionized water. 75 µL of internal standard stock solution (hexane) and 125 µL of absolute ethanol (EtOH) was added to give a final solution of 5 mL. This mixture was immediately sealed with a magnetic cap and mixed. Using the AOC 5000 Autosampler, the vials were pre-incubated at 65°C for 10 minutes before the introduction of a SPME fibre (65 µm, PDMS/DVB) into the headspace of the vial and incubated at 65°C for 15 minutes. The SPME fibre was then inserted into the injection port and desorbed for 5 minutes. The GC-MS instrument used in this analysis was the Shimadzu QP2010 Ultra GC-MS with a split/splitless injector equipped with a HP5MS column (30 m $\times$ 0.25 mm diameter) and positive electron ionization detector. The operating conditions were as follows: column temperature initially at 55°C for 2 min, then 55–180 °C at 6°C/min, followed by holding at 180°C for 1 min; injector temperature at 250°C, detector temperature at 200°C; and carrier gas He 1.0 mL/min. The mass spectrometer settings were as follows: positive electron ionisation mass spectra (EI-MS) as the selected ionisation mode with an ionisation energy of 70 eV at a scan rate of 2 scans per second.

3.3.3 Nucleic acid extraction

In this study, xanthogenate DNA extraction was selected because it has successfully been used to isolate DNA from a diverse range of microorganisms and environmental samples (Tillett & Neilan, 2000). This method uses potassium ethyl xanthogenate which forms water-soluble polysaccharide xanthates. These xanthates disrupt the cell walls and bind with amine-containing groups to give insoluble complexes that are consequently precipitated. This avoids the use of toxic chemicals, while the xanthate-binding of metals

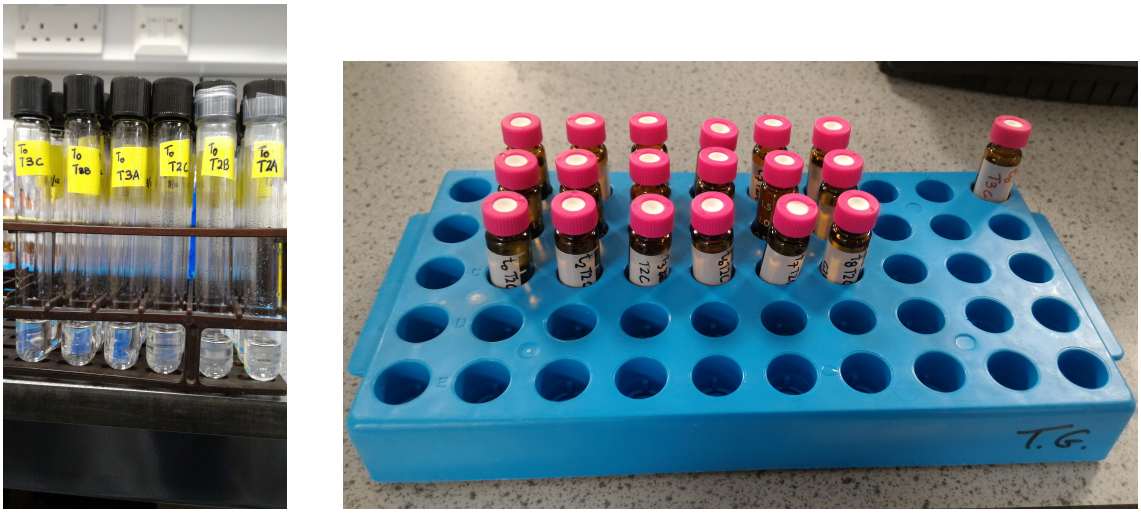

Figure 3.3: Ethyl acetate extraction of ^{12}C-enriched and acid-inhibited sets in triplicate test tubes

can prevent inhibition of the RNA degrading enzymes (Tillett & Neilan, 2000). In general, 1% XS buffer is prepared fresh and added to cell pellets, vortexed, and incubated at 70°C for up to 120 minutes depending on the sample. The tubes are placed on ice and then centrifuged to remove the cell debris. The supernatant is transferred to fresh tubes containing precipitation media to precipitate the DNA. The mixture is then centrifuged to remove the supernatant, washed with ice-cold ethanol, air-dried, and then re-suspended in Tris-HCl and EDTA (TE) buffer.

Whole DNA from the SIP flasks was extracted as described by Tillett and Neilan (2000). Briefly, cell pellets were obtained by centrifugation at 13,000 revolution per minute (rpm) in 1.5-mL Eppendorf tubes and stored at −20°C until extraction. For DNA extractions, the cell pellets were re-suspended with 50 µL TER Buffer (10 mM Tris-HCl, pH 7.4; 1 mM EDTA, pH 8; 100 µg/mL RNAseA). 750 µL of freshly prepared 1% XS buffer (1% potassium ethyl xanthogenate; 100 mM Tris-HCl, pH 7.4; 20 mM EDTA, pH 8.0; 1% sodium dodecylsulfate; 800 mM ammonium acetate) was then added and mixed for 10 s by inversion. The tubes were incubated at 70°C for 30 min. After incubation, the tubes were placed on ice for 30 min to precipitate cell debris. The precipitated cell debris was then collected by centrifugation (13,000 rpm for 10 min). The supernatant from each tube

was dispensed into fresh 2.0-mL Eppendorf tubes containing 750 µL 100% isopropanol and allowed to stand for 10 min to allow DNA to precipitate. Precipitated DNA was then pelleted by centrifugation (13,000 rpm for 10 min) and the supernatant discarded. The DNA pellets were later washed with 750 µL of ice cold 70% EtOH, centrifuged for 10 minutes and the supernatant discarded. The pellets were vacuum-dried for at least 30 min and re-hydrated in 50 µL TE buffer (10 mM Tris-HCl pH 7.4; 1 mM EDTA, pH 8) overnight. The extracted DNA was then verified on 1% agarose gel electrophoresis with GelRed™ nucleic acid stain at 80 V for 30 minutes using HINDIII ladder as the DNA marker. The re-hydrated DNA samples were stored at −20°C before the commencement of the next steps.

3.3.4 Gradient fractionation and identification of ^{13}C-enriched DNA

Cesium chloride (CsCl) stock solution of a desired concentration was prepared. DNA and the CsCl stock solution are then mixed and transferred into an ultracentrifugation or polyallomer tubes. SYBR Safe™ is added and the tube balanced and sealed. These tubes are then ultracentrifuged at high speed, for at least 40 h.

SYBR Safe™ is a safer alternative to ethidium bromide (EtBr) as a nucleic acid stain, used to visualize separated DNA bands. It was introduced to replace the highly mutagenic EtBr which makes the procedure less desirable (Chen et al., 2010; U. Edinburgh Health & Safety Department, 2016; Uhlík et al., 2009). In addition, the use of UV to observe the bands may also damage the DNA for the downstream process (Uhlík et al., 2009). In order to avoid the use of ultraviolet light, a blue-light transilluminator is used.

Following ultracentrifugation, gradient fractionation and DNA precipitation are carried out. This requires collecting fractions in small volumes in order to separate the ‘heavy’ and ‘light’ DNA. Fractions are then precipitated to remove the SYBR Safe™ nucleic acid stain and recover the DNA.

More specifically, to separate ^{13}C-enriched DNA from non-enriched DNA, CsCl gradient ultracentrifugation was performed as previously described by (Martineau et al., 2008).

For this, CsCl stock (ca 1.72 g/mL) was first prepared by dissolving CsCl in TE buffer. 6 mL of the stock was then added to each polyallomer tube and then 50 µL of the total DNA extracted from the previous step was added into each polyallomer tube followed by the addition of 8 µL of 10,000× SYBR Safe™ nucleic acid stain and 2 µL of purified *Escherichia coli* DNA that was grown on ^{12}C-glucose as an internal standard. The tubes were mixed gently and then filled with more CsCl stock solution to at least 75% capacity. The polyallomer tubes were balanced using the CsCl stock solution to a maximum mass difference of 0.05 g. The remaining volume of the polyallomer tubes was filled with mineral oil (Beckman) and balanced again to a maximum mass difference of 0.05 g. Any bubbles were gently removed, and the tubes were crimp-sealed using a Beckman Coulter Cordless tube-topper for ultracentrifugation (see Figure 3.4). The tubes were ultracentrifuged in a 70.1 Ti rotor at a speed of 43,500 rpm at 20°C in vacuum for 40 hours in the Beckman Coulter Optima L-100 XP ultracentrifuge. When the run was completed, the tubes were gently removed and DNA separation was observed using a blue light transilluminator in order to observe for any blue-green bands that are indicative of DNA. The band containing 'light' unlabelled DNA was expected to be higher up the polyallomer tube compared to the 'heavier' ^{13}C DNA band. If bands were visible, their positions were marked to facilitate the gradient fractionation step. Up to 50 fractions of 125 µL each were collected from each sample and the refractive index of each fraction was measured using a Reichert AR200 Digital Refractometer.

3.3.5 SYBR Safe removal and DNA quantification

To remove SYBR Safe™, DNA from each fraction was recovered by ethanol precipitation (Sambrook et al., 1989). To each fraction (ca 125 µL) in 2-mL Eppendorf tubes, 1375 µL of 72.9% EtOH was added, mixed gently, and left at 4°C overnight. The tubes were then centrifuged at 14,000g for 15 minutes at 4°C. The supernatant was then carefully decanted and the pellet washed with 800 µL of 70% EtOH and centrifuged again at 14,000g for 5 minutes at 4°C. The supernatant was removed and the tube allowed to dry under low vacuum to remove any remaining EtOH. The DNA in each tube was then re-hydrated

Figure 3.4: Left: Ultracentrifugation tubes comprising cesium chloride stock solution, enriched DNA and *E. coli* internal standard. Right: Beckman Coulter ultracentrifugation machine used in this study

in 50 µL TE buffer and stored until further use. DNA concentration was then quantified using a NanoDrop ND-3300 Fluorospectrometer (Thermo) and Quant-iT™ PicoGreen™ dsDNA Kit (Invitrogen) which can detect dsDNA concentrations as low as 25 pg/mL in the presence of ssDNA, RNA, and free nucleotides.

3.3.6 Denaturing gradient gel electrophoresis

DGGE is a molecular fingerprinting method used to separate polymerase chain reaction (PCR)-generated DNA. This method separates DNA products based on the varying denaturing characteristics of individual DNA molecules. This circumvents the problem faced with conventional agarose gel electrophoresis which only exhibits a single band for bands of a similar size since it cannot discriminate DNA based on the domains. DGGE overcomes this by varying the concentrations of chemical denaturant (a mixture of urea and formamide) as the DNA products migrate through the polyacrylamide gel. Separation depends on the

Table 3.2: Primer used for DGGE-PCR (Mühling et al., 2008; Wang et al., 2008; Muyzer et al., 1993)

Primers	Length	Sequences of primers
341f-GC	341-357	5'-CCT ACG GGA GGC AGC AG-3'
534r	517-534	5'-ATT ACC GCG GCT GCT GG-3'

decreased electrophoretic mobility of a partially melted double-stranded DNA molecule, brought about by variations in base sequences causing the melting point to differ (Muyzer & Smalla, 1998). Since sequences tend to vary in bases, sequences with lower GC contents have a lower denaturing point. Weaker bases denature first, causing them to migrate more slowly. When DNA fragment reaches a denaturing point in the denaturing gel, the DNA molecule undergoes a transition from a helical to a partially denatured molecule, thus impeding further migration of the fragment down the gradient (Muyzer & Smalla, 1998). This produces varying patterns which can be used to represent a certain bacterial population. Fingerprints from a certain population can then be uploaded into the database for various analysis, for example, to investigate broad phylogenies (Laboratory for Microbial Ecology, University of Toledo, 2004).

Selected fractions were then analysed by DGGE to visualize the separation of DNA. For this, polymerase chain reaction (PCR) amplification of the fractions was performed with Veriti 96 Well Thermal Cycler (Applied Biosystem) using 1 µL of DNA from each fraction per 25 µL PCR mixture. The primers used for the PCR were 341f-GC clamp and 534r (4 pmol/L) (see Table 3.2). The GC clamp comprised 40-base pairs: 5'-CGC CCG CCG CGC GCG GCG GGC GGG GCG GGG GCA CGG GGGG-3' (Mühling et al., 2008; Wang et al., 2008; Muyzer et al., 1993). The PCR cycle was carried out as follows: 94°C for 5 min, followed by 28 cycles of 94°C for 1 min, 64°C for 1 min, and 72°C for 1.5 min and a final extension step of 72°C for 10 min. PCR products were confirmed on a 1.5% (w/v) agarose gel alongside a Quickload 100bp and 1kb ladder (New England Biolabs). The amplified products were then separated on a 6% acrylamide gel with a denaturant range of 30–70% (80% denaturant contains 5.59 M urea and 32% (v/v) molecular grade formamide). Electrophoresis was run at a constant voltage of 60 V for 16 h at 60°C in 1× TAE Buffer

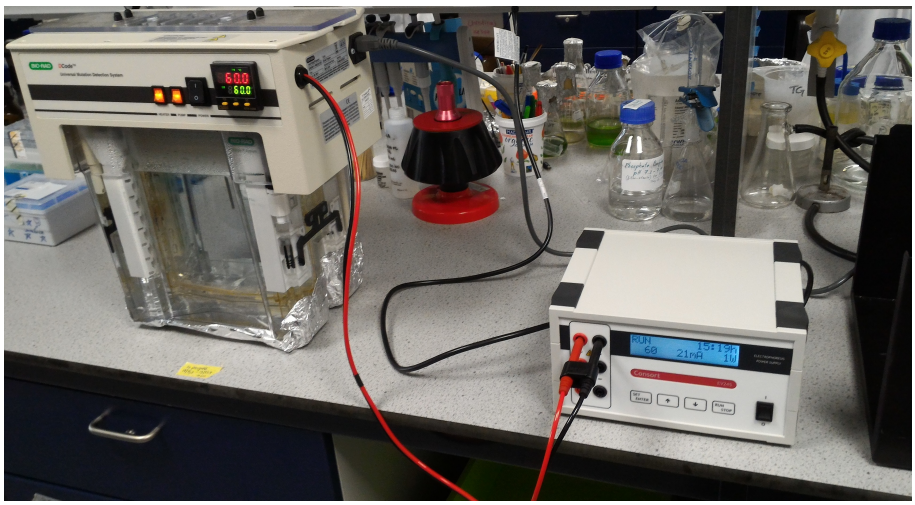

Figure 3.5: DGGE setup with the gel attached to the core assembly immersed in ca 7 L 1× TAE buffer

on the DCode Universal Mutation Detection System (Biorad) (see Figure 3.5). After electrophoresis, the gels were stained with SYBR Safe™ at 1:10,000 dilutions for 15 min and scanned with Genesys Gel Imager. Gel image colours were inverted and adjusted for contrast.

Chapter 4

Results and Discussion

4.1 Degradation of hexadecane during SIP

Oil spills in marine waters are a cause of great concern given their public and ecological impact. Alkanes tend to form the bulk of the crude oil extracted and therefore their influence on the environment based on their sheer volume could still pose a serious environmental challenge if not immediately removed. Hexadecane, a medium-length aliphatic hydrocarbon, is one of the most common hydrocarbon found in crude oil and hence is usually used as a model substrate in bioremediation-related studies.

Experiments were conducted to determine the potential of the diatom-associated bacterial community in the ^{12}C-enriched experimental set that can degrade hexadecane. ^{12}C-hexadecane was selected for degradation profile to allow for a parallel comparison with the ^{13}C-hexadecane.

During the SIP experiment, incubations containing the unlabelled *n*-hexadecane and the acid-inhibited control were run in parallel to measure for the disappearance of the hydrocarbon due to its assimilation by the microbial community. The endpoint selected for this experiment was 8 days to allow sufficient incorporation of the ^{13}C. As shown in Figure 4.1 (left panel), ^{12}C-hexadecane incubations showed significant levels of degradation, with almost all the hexadecane degraded by day 8. The ^{12}C cultures began to degrade hexadecane after 2–3 days. We observed that the ^{12}C cultures might have exhibited a

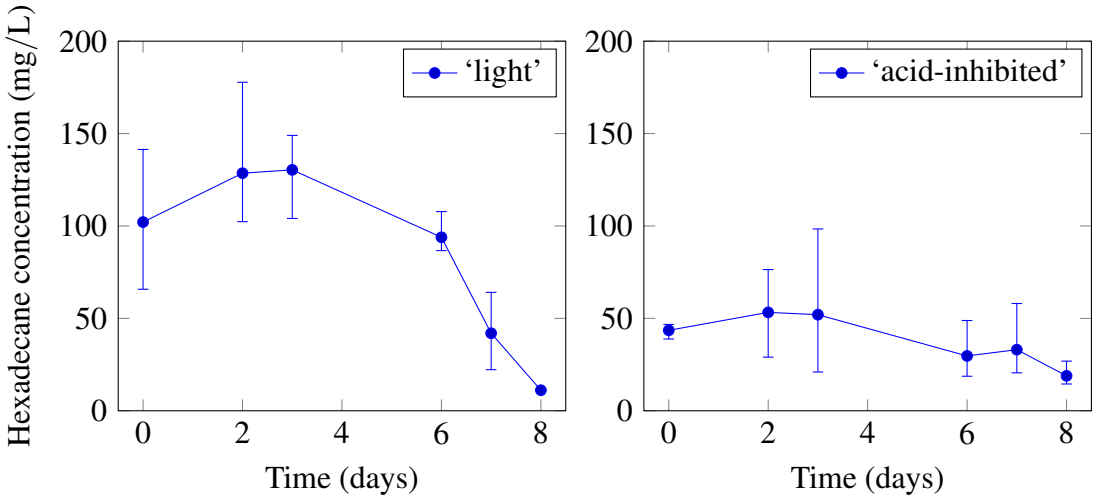

Figure 4.1: Time course of ^{12}C-hexadecane degradation in both sets of triplicate setups. 'Light': cultures amended with unlabelled hexadecane, 'acid-inhibited': cultures amended with unlabelled hexadecane and phosphoric acid to serve as the acid-inhibited controls. The endpoint for this incubation was determined to be 8 days. Error bars are from triplicate samples.

lag phase of at least two days before significant degradation was observed. Moreover, as mentioned by (Gutierrez, Singleton, et al., 2013), achieving sufficient incorporation of the labelled carbon within short incubation times is desirable. Hence, based on the significant degradation of the ^{12}C-hexadecane, the 8-day duration of the SIP incubation using ^{13}C-hexadecane would likely produce a similar degradation profile. A similar set of experiment by (Mishamandani et al., 2014) exhibited comparable duration of degradation although complete degradation was observed by day 5. A study by Sheppard et al. (2013) with the addition of 65 µL of ^{12}C-hexadecane or ^{13}C-hexadecane per litre of culture showed 36.9–43.2% degradation of the hydrocarbon after 72 hours of incubation. Therefore, since this experiment started with an initial added volume of 8 µL of ^{12}C-hexadecane (ca 160 µL per litre of seawater), complete degradation of *n*-hexadecane was likely to be longer. It is also possible that, as the substrate concentration used in this study was comparatively higher, there might have been a longer initial lag phase for degradation (Maier, 2014). If the Monod equation (which describes the relationship between the substrate concentration and specific growth rate) applies, there is a possibility that the higher substrate concentration

might have influenced the specific growth rate (Maier, 2014). It is also worthy to consider the possibility of cross-feeding on ^{13}C-labelled by-products, intermediates, or dead cells if these cultures were allowed to run for longer periods of time. This might result in the distribution of the ^{13}C amongst other members of the bacterial community which are not directly involved in ^{13}C-hexadecane degradation (Mishamandani et al., 2014). However, the probability of cross-feeding occurring is relatively low since the experiment was only ran for 8 days.

The acid-inhibited set of this experiment (Figure 4.1, right) serves as the negative incubation control which involved addition of phosphoric acid to inhibit any possible degradation by the bacteria. Concentrations of hexadecane degradation are therefore expected to be unchanged throughout the experiment, with concentrations similar to that of the ^{12}C-hexadecane set at the start of the experiment (i.e., 120 mg/L). Unfortunately, due to prolonged storage times, the GC-MS results for the negative control proved inconclusive. GC-MS quantification of the acid-inhibited samples showed that hexadecane concentrations were constantly lower than that of the ^{12}C-enriched samples. This was probably attributed to the long storage times between sampling and GC-MS analysis. It was observed that after prolonged storage of the ethyl acetate triplicate test tubes, the organic and aqueous phase seemed to have merged. The ethyl acetate upper layer might have evaporated, degraded, or reacted and thereby causing the merger with the aqueous phase (Lyznicki Jr et al., 1974). Presence of phosphoric acid and a low pH of less than 2 might have acted as a catalyst to promote the degradation or reaction between the two phases resulting in the loss of the hexadecane.

4.2 Nucleic acid extraction of ^{13}C-enriched samples

As previously mentioned, for the DNA-SIP experiment, the four flasks which were each sacrificed on days 2, 3, 6, and 8 were labelled samples T1A, T1B, T1C, and T1D respectively. The cell pellets were collected by centrifugation at 14,000 rpm to remove

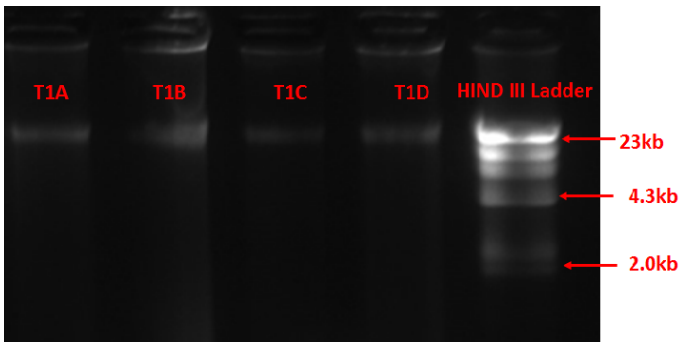

Figure 4.2: DNA isolated from ^{13}C-labelled hexadecane incubations. 1 µL of XS isolated genomic DNA electrophoresed on a 1% agarose gel in 1 × TAE Buffer with 1 µL of λ HindIII DNA marker (lane 5). All gels were stained with SYBR Safe™ and photographed under UV transillumination

Table 4.1: Qualitative cell pellet comparison. Pellet size is determined by visual comparison relative to the smallest pellet

Sample	Time point (day)	Pellet size
T1A	2	++
T1B	3	+++
T1C	6	+
T1D	8	++

supernatant containing the substrates and stored at 4°C. Nucleic acid was then extracted using the xanthogenate extraction (XS) method.

The XS DNA isolation method has previously been successful in isolating high-quality DNA from Gram-negative and Gram-positive bacteria (Tillett & Neilan, 2000). The advantage of the XS buffer is that it does not contain hazardous chemicals, is relatively inexpensive, keeps sample handling to a minimum, and avoids the use of mechanical homogenization processes (Tillett & Neilan, 2000).

The XS extracted DNA was verified on a 1% agarose in 1× tris-acetate-EDTA (TAE) buffer and found to be free from RNA (see Figure 4.2). This was in agreement with recommendations by Tillett and Neilan (2000) which was to resuspend the cell pellet in 50 µL TER buffer prior to the addition of XS buffer. Based on observations on cyanobacterial cultures by Tillett and Neilan (2000), there may be a good correlation between culture density

and biomass yield. If true, we would expect the amount of DNA extracted to be related to the size of pellet obtained (i.e., based on cell pellet size: T1B > T1A = T1D > T1C) (see Table 4.1). However, it is also likely that nucleic acids from the samples were not completely extracted. This is because the protocol recommends incubating 1–2 mL of sample in 750 µL of XS Buffer, while the cell pellet obtained from each sacrificed flask was collected from the centrifugation of 50 mL of culture each. Cell pellets derived from larger-volume cultures may have resulted in a less-than-optimal nucleic acid extraction. This could have been caused by a saturation of the xanthate-bound complexes as well as incomplete cell lysis. The presence of a high number of cell debris may also increase the surface area at which the DNA-could rebind after vortex. These combination of factors could explain why the resultant nucleic acid obtain was not as much as initially expected. Desirably, these would have appeared as bright bands on the 1% agarose gels at the 23 kb mark. Nevertheless, our agarose gel confirmed that the isolation method employed was successful (see Figure 4.2). DNA extracts from samples T1A-D were then subjected to ultracentrifugation to isolate the 'heavy' DNA for subsequent analysis.

4.3 Separation of 'light' and 'heavy' DNA samples

Density gradient ultracentrifugation was performed with 1.72 g/mL CsCl stock solution. The procedures for ultracentrifugation were adapted from (Martineau et al., 2008; Dunford & Neufeld, 2010; Neufeld, Vohra, et al., 2007). Unlike both protocols which used vertical rotors Vti 65.2 and 80 (Beckman), this was adapted to suit the 70.1 1Ti fixed-angle rotor which was the only rotor available for this experiment. According to (Neufeld, Vohra, et al., 2007), any rotor can be used as long as the diffusion gradient are adequately steep so as to sufficiently separate the small difference in buoyant density between the labelled and unlabelled DNA ($\leq 0.04\,\mathrm{g/mL}$). As recommended by Martineau et al. (2008), SYBR Safe™ (Invitrogen, CA) was used to replace EtBr as a nucleic acid stain in the density gradient ultracentrifugation step. SYBR Safe™ has been classified as non-hazardous and visual-

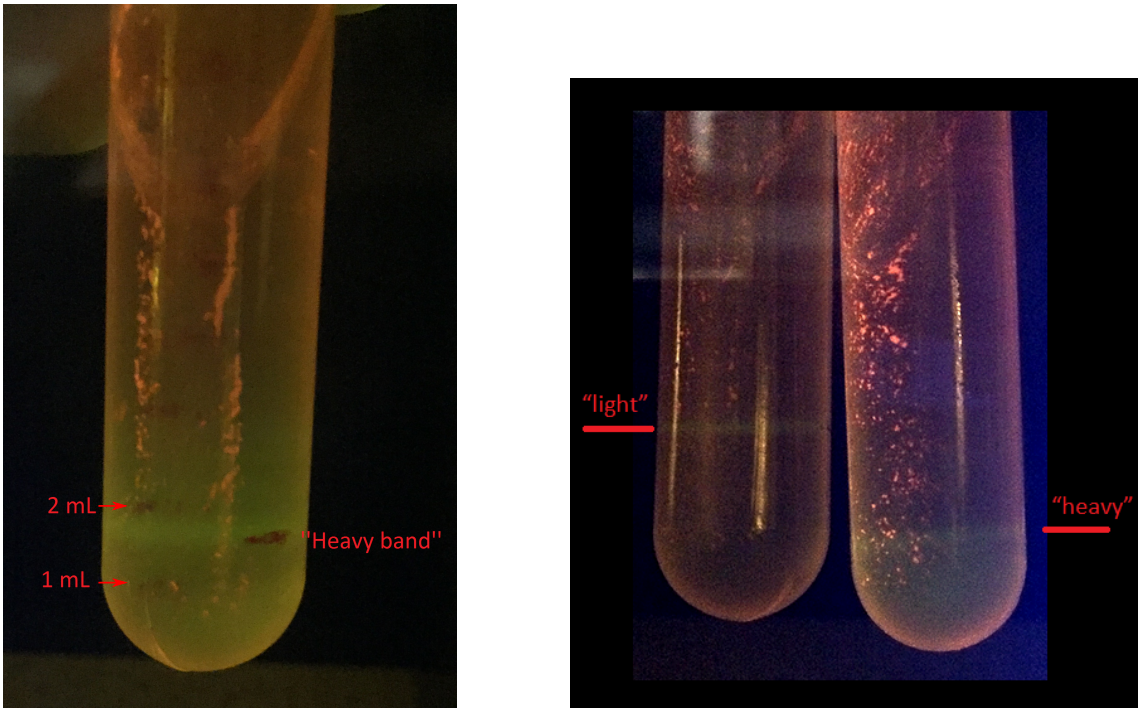

Figure 4.3: Post-ultracentrifuge tube as seen under the blue light transilluminator. The 'heavy' band appears between the 1mL and 2mL tube markings as shown. This was based on earlier practice runs using tubes of *E. coli* grown on ^{12}C-glucose and ^{13}C-glucose. Intensity of bands depend on the amount of DNA present, and therefore, without sufficient DNA, the DNA banding would not be visible.

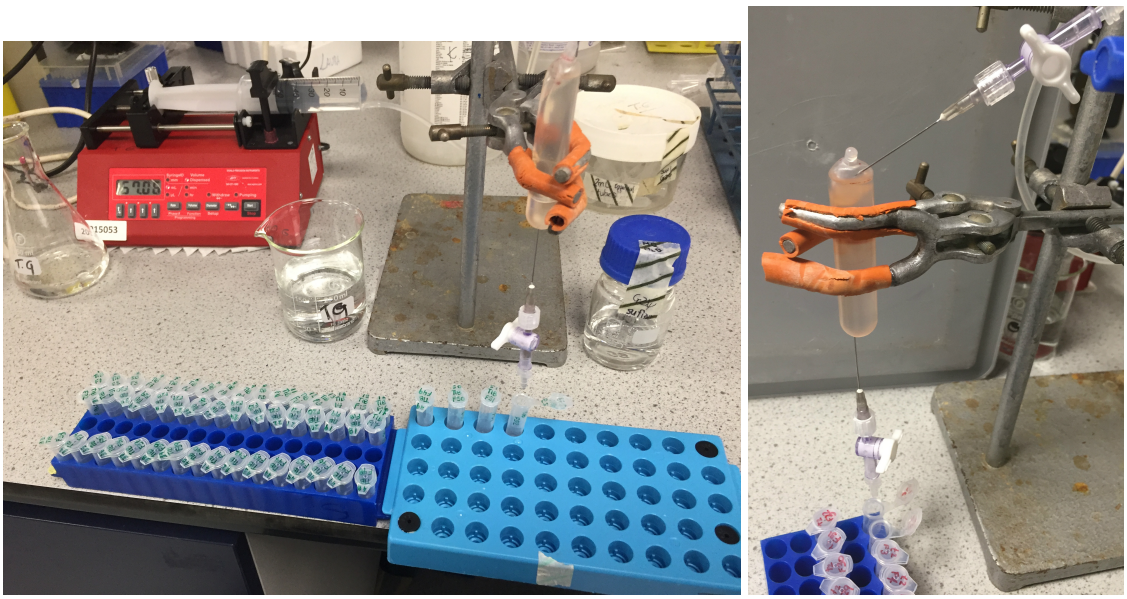

Figure 4.4: Gradient fractionation setup. This method is used to recover DNA from the ultracentrifuge tubes. NE-1000 Programmable Single Syringe Pump was used to retrieve equal volumes of density gradient fractions from ultracentrifuge tubes. For each sample tube, 50 sterile 2-mL microcentrifuge tubes labelled with sample and fraction number (1–50; heavy to light) were prepared. The pump rate was set to retrieve about 5 drops per tube (ca 125 µL).

.

ization of the tubes post-run can be carried out optimally using Safe Imager blue light transilluminator that does not damage DNA.

Density gradient ultracentrifugation is expected to show a separation of labelled and unlabelled DNA based on differences in gradient. While complete resolution of this separation would be desirable, band intensity depends on the amount of genomic material (specifically DNA) present. For example, an ultracentrifugation run using DNA from *E. coli* grown on ^{13}C-glucose and ^{12}C-glucose showed a clear differentiation in the location of the ‘heavy’ and ‘light’ bands in CsCl gradient (see Figure 4.3). However, in the runs with samples T1A-T1D, we found that not all of the 4 tubes showed a pronounced ^{13}C and ^{12}C DNA banding. Bands were either faint or not as pronounced, and hence interpretation of band presence solely on visual inspection was difficult. Therefore, regardless whether the bands are visible or absent under blue light, gradient fractionation was done to confirm gradient formation and separation of ‘heavy’ and ‘light’ DNA (see Figure 4.4).

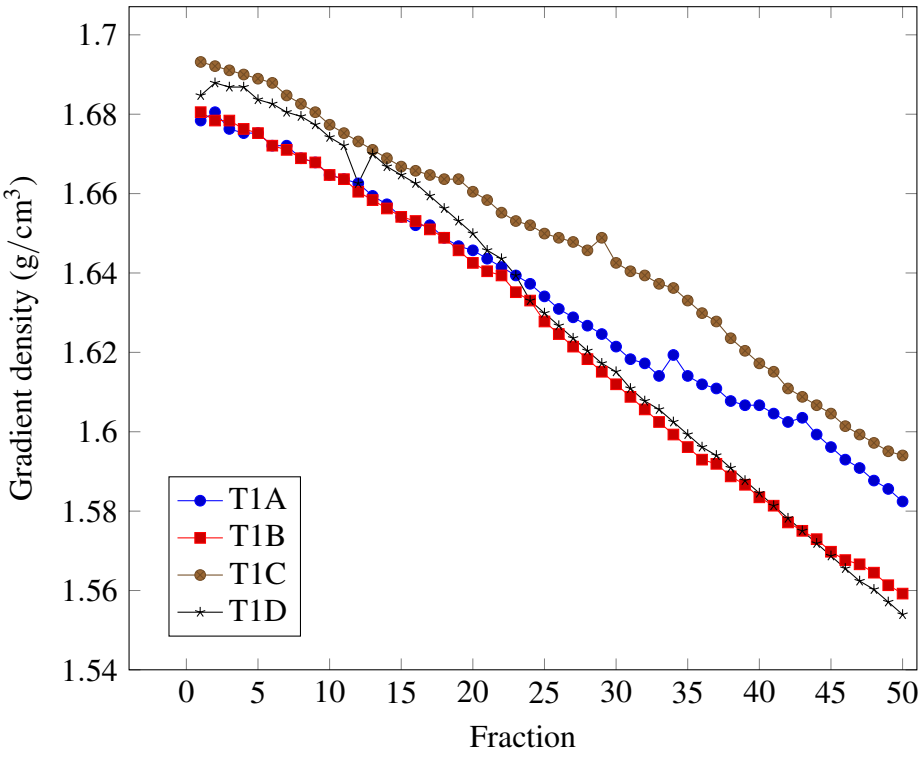

Figure 4.5: Density measurements for T1A–D gradient fractions

4.4 Quantitative analysis of DNA-SIP gradient fractions

Fractions obtained from each gradient were measured for their density using a digital refractometer. As the digital refractometer gives refractive index measurements, these values were converted into corresponding density values based on a CsCl calibration curve by (Beckman Coulter, 2007). The fraction densities were then plotted to verify if a proper gradient had been formed. Measurements for samples T1A–D (see Figure 4.5) confirmed the formation of a proper density gradient with a range of 1.55 to $\sim$ 1.69 g/cm^3 . It is worth noting that gradient density of T1C were relatively higher than the other three samples. The ultracentrifuge run for this sample was repeated as we suspected that the gradient formation had been perturbed, due to the tube having been accidentally dropped. The content of this tube was transferred into a new polyallomer tube and re-ultracentrifuged as before. After ultracentrifugation and fractionation, measurement of the fractions from

the tube showed that a gradient had formed at a range within the values expected. DNA in each fraction was then recovered by ethanol precipitation and re-suspended in 50 µL TE buffer (Jones et al., 2011; Sambrook et al., 1989).

Following gradient fraction measurement, we quantified DNA concentration using the Quant-iT™ PicoGreen™ dsDNA Assay Kit (Invitrogen, USA). Values are represented as a plot of DNA concentration versus fraction in Figure 4.6; note the logarithmic scale on the y-axis. This figure summarizes the overall distribution of the DNA concentration in each of the gradient derived from the four time points. The concentration in sample T1B, which was the flask sacrificed on Day 3, is relatively higher than the rest of the samples. On the contrary, DNA concentration for fractions derived from T1C is generally much lower compared to the fractions from the other samples. In summary, an increase in DNA concentration is probable from T1A (Day 2) to T1B followed by a possible decrease in concentration towards T1D (Day 8). It is worth noting, however, that the concentration obtained from sample T1C might have been affected from the fall and repeat run. Based on this plot, we deduce that the fractions that are likely to contain the ^{13}C would be between fractions 10 and 16. DGGE is planned to be used to verify the position of the ^{13}C-hexadecane fractions and the unlabelled *E. coli* DNA which was used as an internal control in all four ultracentrifugations.

4.5 Analysis of the microbial population by DGGE

To analyse the community profile of the samples on exposure to ^{13}C-hexadecane, we used DGGE to visualize the differences in band separation by DGGE gel. Unfortunately, due to time constraints and availability of the primers, we have decided to select only certain fractions from a specific time point for the DGGE run to demonstrate the genetic diversity of the complex microbial population that are associated with the diatom *Skeletonema costatum* which are capable of degrading hexadecane. We have selected the sample at day 8 (T1D) since it has shown a significant assimilation of ^{13}C in the DNA. From this

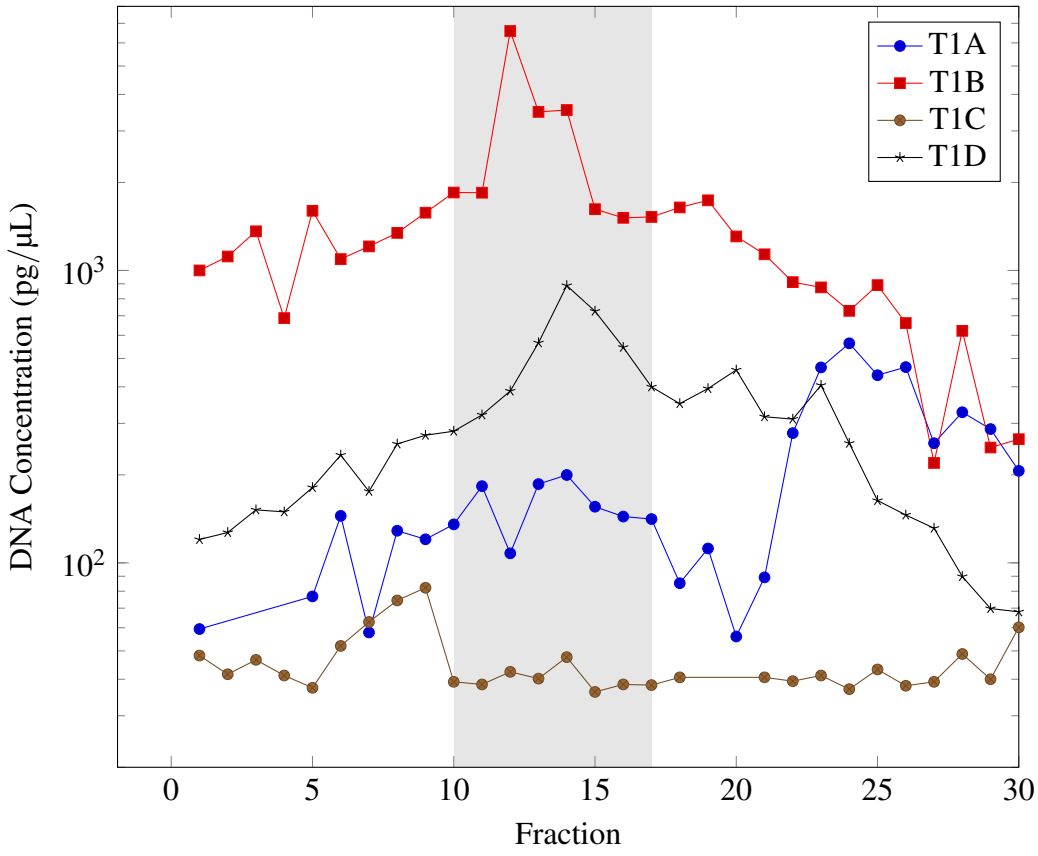

Figure 4.6: Distribution of the 'heavy' and 'light' DNA in SIP fractions from samples T1A–T1D. DNA concentrations are represented on a semi-log plot. Range of fractions believed to contain the highest proportion of ^{13}C-enriched 'heavy' DNA are likely to be in the shaded region.

Table 4.2: T1D fractions selected for PCR-DGGE. Fractions 13–16 are likely to contain the ^{13}C-enriched DNA while fractions 21–24 are likely to comprise other DNA including the *E. coli* internal standard. Fractions 1–2 and 29–30 had trace amounts of DNA and were selected to compare the type of DNA banding present at different fraction numbers.

Fraction	**DNA concentration** (pg/µL)	**Intensity of band vs *E. coli* standard**
1	120.2	-
2	127.0	-
13	565.6	+++
14	887.6	+++
15	725.6	+++
16	545.8	+++
21	316.0	+++
22	310.2	+++
23	404.8	+++
24	256.4	+++
29	69.8	+
30	68.0	+

sample, 12 fractions were chosen based on differences in the type of DNA incorporated ('labelled' or 'unlabelled') and concentration (see Table 4.2).

Before DGGE, PCR amplification was done on the 12 selected fractions and *E. coli* internal standard. One primer pair was used to amplify the genomic DNA sample from the selected fraction by PCR (see Table 3.2). V3 regions of 16S rRNA gene were amplified in the Veriti 96-Well Thermal Cycler (Applied Biosystems) with a desired target band between 200 and 300. PCR was also done on *E. coli* as DNA control using the same set of primers. PCR product was then verified on 1% agarose gel with SYBR Safe™ nucleic acid stain to verify if the PCR products are of similar size (see Figure 4.7). The amplified products were then loaded individually onto the DGGE wells to separate the bands based on sequence differences. The PCR products of the selected fractions from sample T1D were then loaded into wells from left to right, in ascending order of fraction number, beginning from fraction 1 (1st well) to fraction 30 (12th well) while the unlabelled *E. coli* used as an internal standard, was loaded on to the well on the extreme right of the gel (see Figure 4.8).

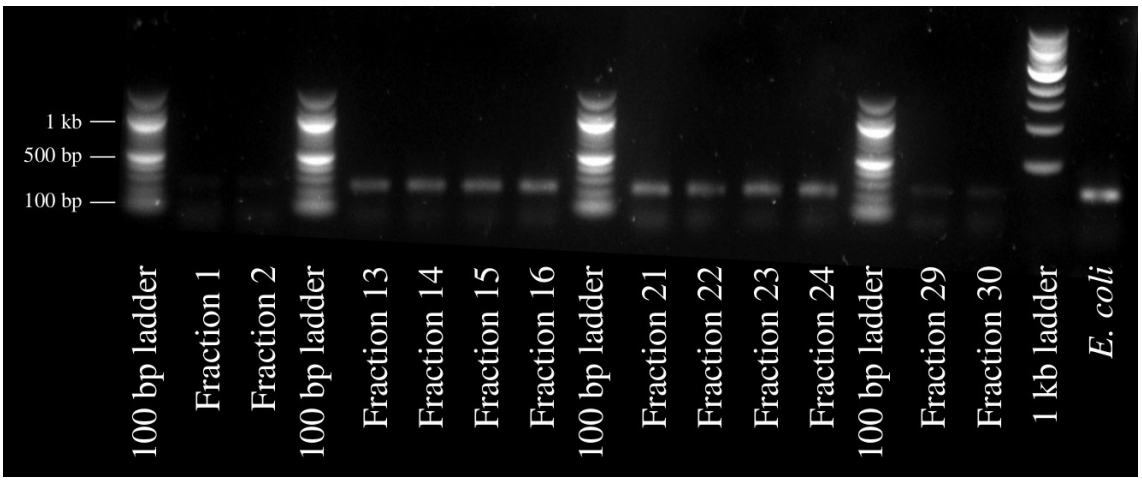

Figure 4.7: Agarose gel electrophoresis of selected fractions from time point T1D.

DGGE allows to identify the members in a community of microorganisms based on the divergence of bacterial species as an indicator of diversity (Muyzer et al., 1993). By visual inspection of the bands on the DGGE fingerprint, this allows an immediate qualitative representation of the diversity of the population and perhaps a semi-quantitative way if relative abundance were to be analysed based on band intensity.

DGGE was then stained with SYBR Safe™ and photographed. Analysis of the bands on the DGGE gel showed substantial separation of the 16S rDNA , with several different banding patterns. The fraction selected for DGGE obtained from sample T1D (day 8) showed clear evidence of the following: (i) isotopic enrichment of DNA in ^{13}C-hexadecane cultures, (ii) separation of ^{13}C-labelled and unlabelled DNA, and (iii) a different banding pattern between these 'heavy' and 'light' DNA fractions. Analysis of the gel found several distinguishable bands in the separation gel, which implies the presence of different bacterial species comprising the community. Fractions 1–2 show at least one band which was very faint. This was expected of the initial fractions in the DGGE, which is usually characterized by traceable amount of DNA. As fraction number increased across the distribution, more bands may appear or disappear, and at varying intensities, depending on the available quantities and sequence. Fractions 13–16, which are the fractions that contain the 'heavy' DNA and at higher concentrations bands showed lesser bands which vary in intensity. At least 5 bands were observed in these wells, which was supposed to be constituents of

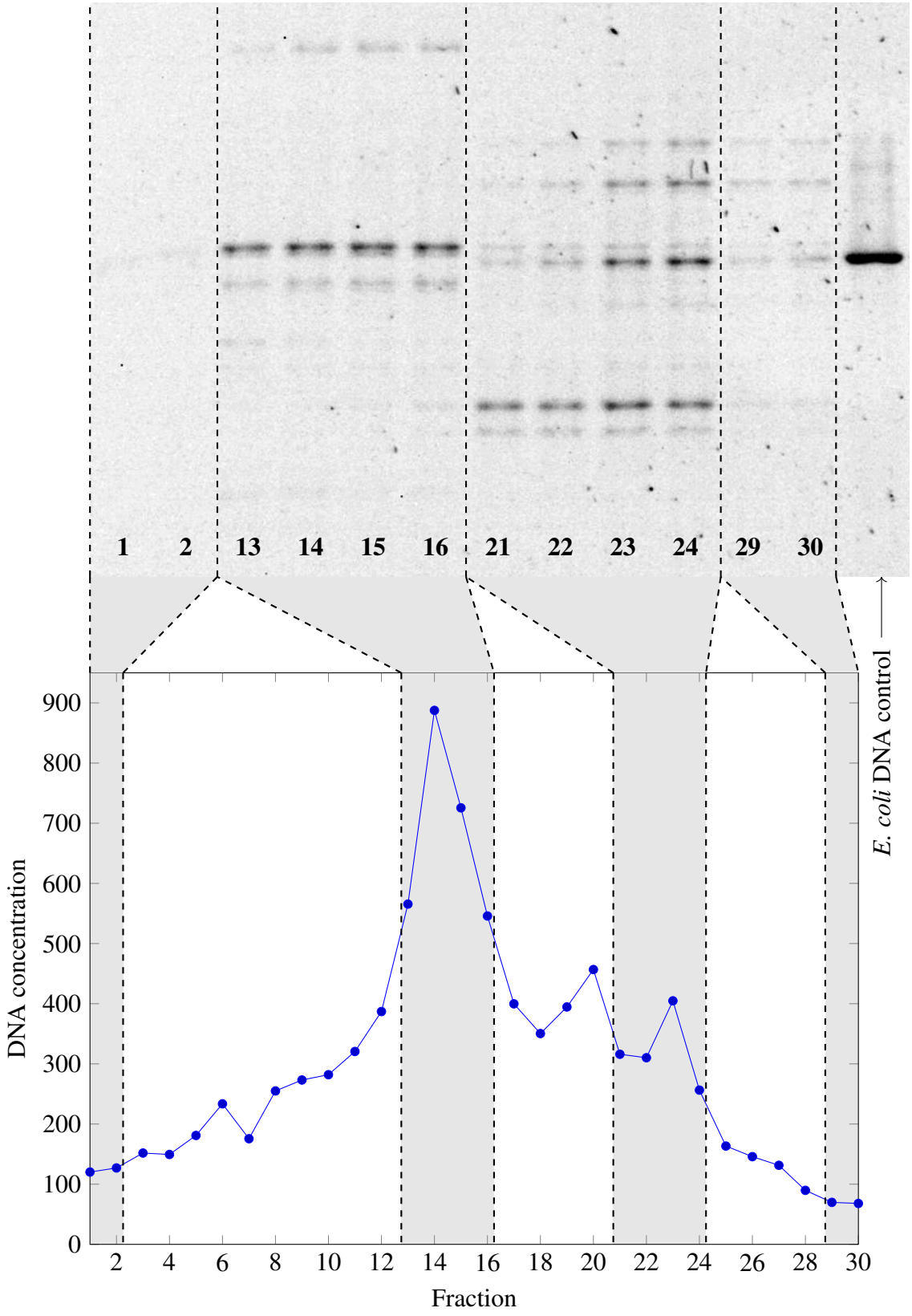

Figure 4.8: Above: DGGE image of bacterial PCR products from selected fractions 1–2, 13–16, 21–24, and 29–30 from T1D sample (day 8); the position of unlabelled *E. coli* DNA is displayed on the right. Below: DNA concentration of sample T1D.

the community that are capable of degrading the ^{13}C-hexadecane. Fractions 21–24 are expected to contain the 'light' DNA, probably belonging to those that are incapable of degrading ^{13}C-hexadecane as well as the *E. coli* grown on ^{12}C-glucose. Noting that 2 µL of the *E. coli* DNA was added into each ultracentrifugation tube, this known standard is used to verify the position of the 'light' DNA in each gradient distribution. This was confirmed with the *E.coli* DNA control that was individually loaded onto a separate well, as a band position indicator on the polyacrylamide gel. Fractions 21–24 shows at least 7 distinguishable bands, which also include the *E. coli* DNA (this appeared as a single bright band on the extreme right lane). Fractions 29–30 shows at least 4 distinguishable bands, some similar to fractions 21–24, albeit much fainter. Based on this DGGE evidence, we imply that there is likely to be different communities associated with the diatom *Skeletonema costatum* which are capable and incapable of degrading hexadecane. Using gradient separation formed during the ultracentrifugation run, we could separate bands by their intensity, which is linked to the number of copies of the product. A successful gradient separation will allow adequate separation of the 'heavy' and 'light' DNA within the fraction. Proper DGGE gradient setup is equally crucial in detection of bands which may differ by several base pairs.

While we can deduce the presence and relative abundance of the bacterial community, we still do not know the bacterial species present in these fractions. Identification may be done through sequencing which will only be done after the completion of this report. Therefore, we do not have at the moment any information on the bacteria involved in the degradation of hexadecane from this SIP experiment with the diatom *S. costatum*.

Chapter 5

Conclusions

5.1 Summary of research achievements

The research presented in this thesis aimed at better understanding the communities of hexadecane-degrading bacteria associated with *Skeletonema costatum*. Specifically we have achieved the following:

1. Hexadecane degradation measurements showed that degradation was almost complete by day 8. This duration of degradation is comparable to those in earlier studies (Sheppard et al., 2013; Mishamandani et al., 2014) which involved media enriched with a lower amount of ^{12}C-hexadecane, confirming the robustness of this experimental setup.

2. Quantitative analysis of DNA-SIP gradient fractions from samples T1A, T1B, T1C, and T1D (corresponding to flasks sacrificed on days 2, 3, 6, 8 respectively) by refractive index measurement confirmed the formation of a proper density gradient within the range expected as mentioned in Section 4.4.

3. DNA concentration of the fractions was compared with the density gradient measurements to deduce the range of fractions which are likely to contain the highest proportion of ^{13}C-enriched DNA, shown in Figure 4.6. This was found to be within the range of fraction 10–15 with the exception of sample T1C which appeared

in fractions 6–9. This was probably due to gradient perturbation caused by the tube being accidentally dropped. The possible range of fraction where the non-enriched ^{12}C-DNA could also be predicted by comparing the distribution against the density measurements. The non-enriched ^{12}C-DNA fractions also contained the ^{12}C-enriched *E. coli* DNA that was added into Tubes 1A, 1B, 1C, and 1D as an internal standard. The range of these 'light' DNA fractions are likely to be between 21–25, with the exception of T1C which is probably between 28–32, again likely due to gradient perturbation.

4. DGGE analysis of the selected T1D (day 8) fractions 1–2, 13–16, 21–24, and 29–30 exhibited several distinct bands in the separation gel, implying the presence of several bacterial species. More bands were observed in the fractions 21–24, which represent communities that are incapable of degrading hexadecane. One of the bands belongs to the ^{12}C-enriched *E. coli DNA* which confirms the position of the 'light' DNA, as shown in Figure 4.8. This band was confirmed by a purified *E. coli* control grown on ^{12}C-glucose that was run in parallel in the DGGE setup.

5.2 Limitations and shortcomings, and how these were addressed

The initial goal of this Master's research was to conduct a DNA-SIP experiment using ^{13}C-hexadecane as substrate.

Within the limitations of the duration of the research, the DNA-SIP study has found that hexadecane has a short removal time span, brought about by a possible consortium of hexadecane-degraders. This consortium has been shown to consist of different constituent members, as visualised by the DGGE analysis; note there are also members that were found uninvolved in the degradation. While more analysis will be done, albeit after the submission of this thesis, we can conclude that significant progress has been made in

achieving the objective of this study. We now discuss the highlights and any limitations of the findings and this work, and recommendations for future studies.

General experimental approach. While the technique involved in the DNA-SIP experiment is well established, as this was the first time that we were conducting the experiment, we decided to validate if each of the post-incubation steps worked. This involved growing cultures of *E. coli* that have been amended with ^{13}C-glucose and ^{12}C-glucose. Whole cells were then collected by centrifugation. This was used as a practice to verify if the following steps work: (i) xanthogenate DNA extraction, (ii) agarose gel electrophoresis, (iii) preparation of the cesium chloride stock solution and the ultracentrifugation run, (iv) removal of the SYBR Safe™ nucleic acid stain, and lastly (v) the DNA quantification step. During the duration of the experiments, we encountered several issues which needed to be addressed. For example, while practising with whole DNA extracted from *E. coli* cultures, this yielded poor quality agarose pictures. It was found that the GelRed™ stain and DNA marker might have degraded. This was confirmed after tests using newly obtained DNA markers and nucleic acid stains. Apart from this, there were also other setbacks which probably consumed valuable time that could have otherwise be spent on the experiment. One of these involved the SYBR Safe™ stain which, after using the stock available for a few runs, was found to be inactive and hence replaced with a fresh batch. Despite this and other minor setbacks, the objectives as originally set out were achieved.

GC-MS quantification approach There are some issues that still need to addressed in the future. For example, the anomaly with GC-MS quantification of the ethyl acetate phase of the 'acid-inhibited' samples needs to be investigated. Addition of 2 mL ethyl acetate to 1 mL of culture would give two immiscible layers, where hexadecane would partition into the upper organic layer due to its non-polar nature. However, as the sample tubes were stored for a prolonged duration of time, there might have been degradation of the hexadecane or chemical reaction between the two phases resulting in the merger of two phases into one single aqueous phase. This phase still persists even with an addition of a fresh volume of ethyl acetate. More interestingly, this was consistent throughout

every sample in the 'acid-inhibited' set of experiments. This would explain why the concentrations of hexadecane were significantly lower at every time point when compared to samples from the 'light' set of experiments. It is therefore recommended to analyse the ethyl acetate samples by GC-MS immediately upon sampling.

DGGE The present study aimed to identify hexadecane-degrading bacteria that are associated with the diatom. This involved analysing the selected ^{13}C-enriched fractions from the four time points by DGGE. However, due to time limitation DGGE was only done on one time point, which was day 8 of the ^{13}C-enriched set. Of these only 12 fractions (1, 2, 13-16, 21-24, 29 and 30) were then chosen for the initial DGGE demonstration (see Table 4.2). Fractions were then amplified by PCR, along with the *E. coli* genomic DNA that was used as an internal standard for this study. Once PCR was complete, DGGE was performed to analyse the bands that would enable us to study the diversity of the community within each fraction. The *E. coli* amplicons were used to confirm the presence of the internal standards as well as to show that the fractions which contained the 'unlabelled' *E. coli* belonged to the 'light' DNA regions. Future work could be planned to perform DGGE on the first 40 fractions of each time point. This would allow for a better assessment of this diversity and how its abundance evolves over time. While DGGE can detect and separate the sequences based its denaturing characteristics, it does not provide information on the identity of the constituents of the population present in each fraction. The inclusion of the *E. coli* as a control for the DGGE can then single out the corresponding band present on the gel and determine the fractions corresponding to the 'light' DNA; in this way, this was the only band on the gel that could be assigned to a bacterial taxon – i.e., to *E. coli*. Identification of the other members of the bacterial community can only be done by sequencing. To do this, it is planned at a later time to pool select 'light' and 'heavy' fractions for every time point and send them for barcoded-amplicon Illumina MiSeq sequencing. Selection of these fractions would be based on the DNA quantification assay which was referenced against the density of the fractions. A total of nine samples for MiSeq sequencing has currently been sent for this type of analysis, as follows: a tube

of pooled fractions representing the ‘heavy’ DNA fractions for each of the 4 time points; the same for the ‘light’ DNA fractions and a sample of whole-DNA extracted from the non-axenic diatom from the start of the SIP experiment.

References

Aeppli, C., Carmichael, C. A., Nelson, R. K., Lemkau, K. L., Graham, W. M., Redmond, M. C., ... Reddy, C. M. (2012). Oil weathering after the Deepwater Horizon disaster led to the formation of oxygenated residues. *Environmental science & technology*, *46*(16), 8799–8807.

Amin, S. A., Parker, M. S., & Armbrust, E. V. (2012). Interactions between diatoms and bacteria. *Microbiology and molecular biology reviews: MMBR*, *76*(3), 667-684.

Andelman, J. B., & Suess, M. J. (1970). Polynuclear aromatic hydrocarbons in the water environment. *Bulletin of the World Health Organization*, *43*(3), 479.

Battelle. (2007). *Sediment toxicity of petroleum hydrocarbon fractions* (Tech. Rep.). Boston, MA, USA: Massachusetts Department of Environmental Protection.

Beckman Coulter. (2007). Density and refractive index for cesium chloride at 25 degrees C. In *Rotors and tubes. For Beckman Coulter J2, J6, and Avanti® J series centrifuges* (p. 134). Beckman Coulter.

Binark, N., Güven, K., Gezgin, T., & Ünlü, S. (2000). Oil pollution of marine algae. *Bulletin of environmental contamination and toxicology*, *64*(6), 866–872.

Chen, Y., Vohra, J., & Murrell, J. C. (2010). Applications of DNA-stable isotope probing in bioremediation studies. *Bioremediation: Methods and Protocols*, 129-139.

Cheng, L., Ding, C., Li, Q., He, Q., Dai, L.-r., & Zhang, H. (2013). DNA-SIP reveals that Syntrophaceae play an important role in methanogenic hexadecane degradation. *PLoS One*, *8*(7), e66784.

D'Auria, M., Emanuele, L., Racioppi, R., & Velluzzi, V. (2009). Photochemical degradation of crude oil: Comparison between direct irradiation, photocatalysis, and photocatalysis on zeolite. *Journal of hazardous materials*, *164*(1), 32-38.

Dunford, E. A., & Neufeld, J. D. (2010). DNA stable-isotope probing (DNA-SIP). *JoVE (Journal of Visualized Experiments)*, *42*.

Fathepure, B. Z. (2015). Recent studies in microbial degradation of petroleum hydrocarbons in hypersaline environments. In *Proc. Halophiles 2013, international congress on halophilic microorganisms* (Vol. 5, p. 35).

Guillard, R. R. L. (1975). Culture of phytoplankton for feeding marine invertebrates. In W. L. Smith & M. H. Chanley (Eds.), *Culture of marine invertebrate animals: Proceedings — 1st conference on culture of marine invertebrate animals greenport* (pp. 29–60). Boston, MA: Springer US.

Guillard, R. R. L., & Ryther, J. H. (1962). Studies of marine planktonic diatoms: I. Cyclotella nana Hustedt, and Detonula confervacea (cleve) Gran. *Canadian Journal of Microbiology*, *8*(2), 229-239.

Gutierrez, T. (2010). Searching for new bacterial species that break down polyaromatic hydrocarbons in coastal and oceanic waters. *Rev. Environ. Sci. Biotechnol*, *14*,

205–209.

Gutierrez, T., Biddle, J. F., Teske, A., & Aitken, M. D. (2015). Cultivation-dependent and cultivation-independent characterization of hydrocarbon-degrading bacteria in guaymas basin sediments. *Frontiers in Microbiology*, *6*, 695.

Gutierrez, T., Green, D. H., Nichols, P. D., Whitman, W. B., Semple, K. T., & Aitken, M. D. (2013). Polycyclovorans algicola gen. nov., sp. nov., an aromatic-hydrocarbon-degrading marine bacterium found associated with laboratory cultures of marine phytoplankton. *Applied and environmental microbiology*, *79*(1), 205–214.

Gutierrez, T., Nichols, P. D., Whitman, W. B., & Aitken, M. D. (2012). Porticoccus hydrocarbonoclasticus sp. nov., an aromatic hydrocarbon-degrading bacterium identified in laboratory cultures of marine phytoplankton. *Applied and environmental microbiology*, *78*(3), 628–637.

Gutierrez, T., Rhodes, G., Mishamandani, S., Berry, D., Whitman, W. B., Nichols, P. D., ... Aitken, M. D. (2014). Polycyclic aromatic hydrocarbon degradation of phytoplankton-associated Arenibacter spp. and description of Arenibacter algicola sp. nov., an aromatic hydrocarbon-degrading bacterium. *Applied and environmental microbiology*, *80*(2), 618–628.

Gutierrez, T., Singleton, D. R., Berry, D., Yang, T., Aitken, M. D., & Teske, A. (2013). Hydrocarbon-degrading bacteria enriched by the Deepwater Horizon oil spill identified by cultivation and DNA-SIP. *The ISME journal*, *7*(11), 2091-2104.

Harayama, S., Kishira, H., Kasai, Y., & Shutsubo, K. (1999). Petroleum biodegradation in marine environments. *J Mol Microbiol Biotechnol*, *1*(1), 63–70.

Head, I. M., Jones, D. M., & Röling, W. F. (2006). Marine microorganisms make a meal of oil. *Nature Reviews Microbiology*, *4*(3), 173–182.

Hollebone, B. P. (2014). The oil properties data appendix. In *Handbook of oil spill science and technology* (pp. 575–681). John Wiley & Sons, Inc.

IARC Monographs, V. . (1989). *Crude oil.* `https://monographs.iarc.fr/ENG/Monographs/vol45/mono45-7.pdf`.

ITOPF. (2011). *Fate of marine oil spills.* `http://www.itopf.com/knowledge-resources/documents-guides/document/tip-2-fate-of-marine-oil-spills/`.

ITOPF. (2016). *Oil tanker spill statistics 2015.* `http://www.itopf.com/fileadmin/data/Documents/Company_Lit/Oil_Spill_Stats_2016.pdf`.

ITRC. (2011). *Stable isotope probing emd team fact sheet–november 2011.* `http://www.itrcweb.org/documents/team_emd/SIP_Fact_Sheet.pdf`.

Jones, M. D., Singleton, D. R., Sun, W., & Aitken, M. D. (2011). Multiple DNA extractions coupled with stable-isotope probing of anthracene-degrading bacteria in contaminated soil. *Applied and environmental microbiology*, *77*(9), 2984–2991.

Joye, S. B., Kleindienst, S., Gilbert, J. A., Handley, K. M., Weisenhorn, P., Overholt, W. A., & Kostka, J. E. (2016). Responses of microbial communities to hydrocarbon exposures. *Oceanography*, *29*(3).

Kostka, J. E., Prakash, O., Overholt, W. A., Green, S. J., Freyer, G., Canion, A., ... Huettel, M. (2011). Hydrocarbon-degrading bacteria and the bacterial community response

in gulf of mexico beach sands impacted by the Deepwater Horizon oil spill. *Applied and environmental microbiology*, *77*(22), 7962–7974.

Kumar, C. S., & Prabu, V. A. (2014). Culture of the phytoplankton Skeletonema costatum, Cleve, 1873. *Int. J. Curr. Microbiol. App. Sci*, *3*(11), 129–136.

Laboratory for Microbial Ecology, University of Toledo. (2004). *Denaturing gradient gel electrophoresis (DGGE).* `http://www.eeescience.utoledo.edu/Faculty/Sigler/Von_Sigler/LEPR_Protocols_files/DGGE.pdf`.

Liu, Z., Liu, J., Zhu, Q., & Wu, W. (2012). The weathering of oil after the Deepwater Horizon oil spill: insights from the chemical composition of the oil from the sea surface, salt marshes and sediments. *Environmental Research Letters*, *7*(3), 035302.

Lyznicki Jr, E. P., Oyama, K., & Tidwell, T. T. (1974). Reactivity of organophosphates. IV. Acid-catalyzed hydrolysis of triethyl phosphate: a comparison with ethyl acetate. *Canadian Journal of Chemistry*, *52*(7), 1066–1071.

Mackelprang, R., & Mason, O. U. (2016). Marine microbiology: Community clean up. *Nature microbiology*, *1*, 16102.

Maier, R. M. (2014). Bacterial growth. In I. Pepper, C. Gerba, & T. Gentry (Eds.), *Environmental microbiology* (3rd ed., chap. 3). Academic Press.

Marchant, R., Sharkey, F. H., Banat, I. M., Rahman, T. J., & Perfumo, A. (2006). The degradation of n-hexadecane in soil by thermophilic geobacilli. *FEMS microbiology ecology*, *56*(1), 44–54.

Martineau, C., Whyte, L. G., & Greer, C. W. (2008). Development of a SYBR Safe™ technique for the sensitive detection of DNA in cesium chloride density gradients for stable isotope probing assays. *Journal of microbiological methods*, *73*(2), 199–202.

McGenity, T. J., Folwell, B. D., McKew, B. A., & Sanni, G. O. (2012). Marine crude-oil biodegradation: a central role for interspecies interactions. *Aquatic Biosystems*, *8*(1), 10.

Mishamandani, S., Gutierrez, T., & Aitken, M. (2014). DNA-based stable isotope probing coupled with cultivation methods implicates methylophaga in hydrocarbon degradation. *Frontiers in Microbiology*, *5*, 76.

Mishamandani, S., Gutierrez, T., Berry, D., & Aitken, M. D. (2015). Response of the bacterial community associated with a cosmopolitan marine diatom to crude oil shows a preference for the biodegradation of aromatic hydrocarbons. *Environmental microbiology*.

Mühling, M., Woolven-Allen, J., Murrell, J. C., & Joint, I. (2008). Improved group-specific PCR primers for denaturing gradient gel electrophoresis analysis of the genetic diversity of complex microbial communities. *The ISME journal*, *2*(4), 379.

Muyzer, G., De Waal, E. C., & Uitterlinden, A. G. (1993). Profiling of complex microbial populations by denaturing gradient gel electrophoresis analysis of polymerase chain reaction-amplified genes coding for 16S rRNA. *Applied and environmental microbiology*, *59*(3), 695–700.

Muyzer, G., & Smalla, K. (1998). Application of denaturing gradient gel electrophoresis (DGGE) and temperature gradient gel electrophoresis (TGGE) in microbial ecology. *Antonie van Leeuwenhoek*, *73*(1), 127–141.

National Academies of Sciences, Engineering, and Medicine. (2016). *Spills of diluted*

bitumen from pipelines: A comparative study of environmental fate, effects and response. National Academies Press.

National Center for Biotechnology Information. (2017). *Hexadecane.* PubChem Compound Database; CID=11006, https://pubchem.ncbi.nlm.nih.gov/compound/11006.

Neufeld, J. D., Vohra, J., Dumont, M. G., Lueders, T., Manefield, M., Friedrich, M. W., & Murrell, J. C. (2007). DNA stable-isotope probing. *Nature protocols*, *2*(4), 860–866.

Neufeld, J. D., Wagner, M., & Murrell, J. C. (2007). Who eats what, where and when? Isotope-labelling experiments are coming of age. *The ISME Journal*, *1*(2), 103.

Office of Response and Restoration, National Oceanic and Atmospheric Administration, University of Toledo. (2015). *How does oil get into the ocean?* http://response.restoration.noaa.gov/about/media/how-does-oil-get-ocean.html.

OPEC. (2017). *Monthly oil market report, 18 january 2017, monetary policies and their effect on the oil market* (Tech. Rep.). Vienna, Austria: Author.

Prince, R. C., Garrett, R. M., Bare, R. E., Grossman, M. J., Townsend, T., Suflita, J. M., ... Lessard, R. R. (2003). The roles of photooxidation and biodegradation in long-term weathering of crude and heavy fuel oils. *Spill Science & Technology Bulletin*, *8*(2), 145-156.

Raj, G. (2009). Advanced physical chemistry. In *Advanced physical chemistry* (pp. 1384–1385). GOEL Publishing House.

Rontani, J., Bosser-Joulak, F., Rambeloarisoa, E., Bertrand, J., Giusti, G., & Faure, R. (1985). Analytical study of asthart crude oil asphaltenes biodegradation. *Chemosphere*, *14*(9), 1413–1422.

Sambrook, J., Fritsch, E. F., & Maniatis, T. (1989). *Molecular cloning: a laboratory manual* (No. Ed. 2). Cold spring harbor laboratory press.

Sheppard, P., Adetutu, E., Young, A., Manefield, M., Morrison, P., & Ball, A. (2013). Stable isotope probing - a tool for assessing the potential activity and stability of hydrocarbonoclastic communities in contaminated seawater. *J. Bioremed. Biodegrad*, *4*(2).

Spaulding, S., & Edlund, M. (2008). *Skeletonema*. In *Diatoms of the united states.* Retrieved from http://westerndiatoms.colorado.edu/taxa/genus/skeletonema

Steering Committee for the Petroleum in the Marine Environment Update, National Research Council. (1985). *Oil in the sea: Inputs, fates, and effects*. National Academies Press.

Tillett, D., & Neilan, B. A. (2000). Xanthogenate nucleic acid isolation from cultured and environmental cyanobacteria. *Journal of Phycology*, *36*(1), 251–258.

Transportation Research Board and National Research Council. (2003). *Oil in the sea III: Inputs, fates, and effects*. The National Academies Press.

U. Edinburgh Health & Safety Department. (2016). *Ethidium bromide.* http://www.ed.ac.uk/health-safety/guidance/hazardous-substances/ethidium-bromide.

Uhlík, O., Jecná, K., Leigh, M. B., Macková, M., & Macek, T. (2009). DNA-based stable isotope probing: a link between community structure and function. *Science of the Total Environment*, *407*(12), 3611–3619.

United States Environment Protection List. (2014). *Priority pollutant list.* https://www.epa.gov/sites/production/files/2015-09/documents/priority-pollutant-list-epa.pdf.

U.S. Congress. (1991). Office of technology assessment, bioremediation for marine oil spills-background paper. *Government Printing Office OTA-BP-O-70*.

U.S. Energy Information Administration. (2016a). *International energy outlook 2016* (Tech. Rep.). Washington D.C., USA: U.S. Energy Information Administration.

U.S. Energy Information Administration. (2016b). *Oil: Crude and petroleum products explained. use of oil.* http://www.eia.gov/energyexplained/index.cfm?page=oil_use.

U.S. Energy Information Administration. (2016c). *What drives crude oil prices? an analysis of 7 factors that influence oil markets, with chart data updated monthly and quarterly* (Tech. Rep.). Washington D.C., USA: U.S. Energy Information Administration.

Verlencar, X., & Desai, S. (2004). *Phytoplankton identification manual.* http://nio.org/userfiles/file/biology/Phytoplankton-manual.pdf.

Wang, J., Ma, T., Zhao, L., Lv, J., Li, G., Liang, F., & Liu, R. (2008). PCR–DGGE method for analyzing the bacterial community in a high temperature petroleum reservoir. *World Journal of Microbiology and Biotechnology*, *24*(9), 1981–1987.

Whitby, C., Bailey, M., Whiteley, A., Murrell, C., Kilham, K., Prosser, J., & Lappin-Scott, H. (2005). Stable isotope probing links taxonomy with function in microbial communities. *Asm News*, *71*(4), 169–173.

World Bank, Development Prospects Group. (2013). *Commodity price forecast update, released: January 15 2013.* http://www.eia.gov/finance/markets/reports_presentations/eia_what_drives_crude_oil_prices.pdf.

Yakimov, M. M., Timmis, K. N., & Golyshin, P. N. (2007). Obligate oil-degrading marine bacteria. *Current opinion in biotechnology*, *18*(3), 257–266.

Yang, T., Nigro, L. M., Gutierrez, T., D'Ambrosio, L., Joye, S. B., Highsmith, R., & Teske, A. (2016). Pulsed blooms and persistent oil-degrading bacterial populations in the water column during and after the Deepwater Horizon blowout. *Deep Sea Research Part II: Topical Studies in Oceanography*, *129*, 282-291.